UNIVERSIDADE FEDERAL DE MINAS GERAIS
PROGRAMA DE PÓS-GRADUAÇÃO EM SANEAMENTO, MEIO AMBIENTE E RECURSOS HÍDRICOS

NANOFILTRATION AND REVERSE OSMOSIS EVALUATION IN GOLD ACID MINE DRAINAGE TREATMENT AIMING WATER REUSE

Alice Oliveira Aguiar

Belo Horizonte
2015

NANOFILTRATION AND REVERSE OSMOSIS EVALUATION IN GOLD ACID MINE DRAINAGE TREATMENT AIMING WATER REUSE

Alice Oliveira Aguiar

Alice Oliveira Aguiar

NANOFILTRATION AND REVERSE OSMOSIS EVALUATION IN GOLD ACID MINE DRAINAGE TREATMENT AIMING WATER REUSE

Dissertação apresentada ao Programa de Pós-graduação em Saneamento, Meio Ambiente e Recursos Hídricos da Universidade Federal de Minas Gerais, como requisito parcial à obtenção do título de Mestre em Saneamento, Meio Ambiente e Recursos Hídricos.

Área de concentração: Meio Ambiente

Linha de pesquisa: Caracterização, prevenção e controle da poluição

Orientador: Míriam Cristina Santos Amaral Moravia

Belo Horizonte
Escola de Engenharia da UFMG
2015

Página com as assinaturas dos membros da banca examinadora, fornecida pelo Colegiado do Programa

AGRADECIMENTOS

São tantas coisas a agradecer que é até difícil saber por onde começar. Agradeço primeiramente à vida, com suas infinitas possibilidades e caminhos misteriosos. A Deus, pela força para seguir em frente sempre lembrando daquilo que nos é mais importante. E por fim, às várias pessoas que direta ou indiretamente trilharam esse caminho comigo.

À Miriam, orientadora dedicada e profissional exemplar. Obrigada pela oportunidade, amizade e confiança durante esses dois anos.

Ao meu marido Luiz Gustavo, por todos os bons momentos, pelo apoio incondicional, pelo amor incalculável. Sou eternamente grata por ter te achado nesse mar infinito de pessoas.

Agradeço aos meus pais, Laura e Orlando, pelo dom da vida e por me guiar tão eximiamente nos seus caminhos. Muito obrigada primeiramente pelos valores ensinados ao longo da vida, pelo incentivo constante para sempre fazer o meu melhor, e pela força nos momentos difíceis.

Ao meu irmão, Marcelo pela constante companhia e ótima amizade. Todos os meus dias não seriam tão divertidos e completos sem você.

À minha avó Hilze. Vó, você é a pessoa mais forte e generosa que conheço; minha inspiração para ser uma pessoa mais solidária e completa. Agradeço por todas as conversas, além da atenção e carinho sempre. Ao meu avô Geraldo, pelo exemplo de vida e de dedicação.

Aos todos os meus tios, tias, primas, primos... Enfim, à minha querida família com seus caóticos encontros familiares e divertidas conversas.

Agradeço às amizades encontradas ao longo de todo esse percurso. Às minhas amigas da engenharia química que viraram amigas da vida: Aline, Barbara Ricci, Barbara Zocratto, Mariana e Lorene. Às minhas amigas desde sempre do colégio Loyola: Ana Clara, Ana Paula, Camilinha, Joana, Natália e Paty.

A todos os companheiros do DESA com quem tive a oportunidade de trabalhar e conhecer. Vocês foram figuras sempre presentes e que me ajudaram a crescer e cresceram comigo nesses últimos dois anos. Agradeço em especial à Laura, pela amizade, positividade, compreensão em momentos difíceis e (n+2) conversas diversas. Ao Wadson e à Luiza, pela dedicação, meticulosidade e atenção, sem vocês não estaria aqui hoje. Ao André, Maria Clara

e Luiza, trabalhos em grupo nunca foram tão perfeitos e ao mesmo tempo divertidos. Enfim, a toda equipe do DESA. Eu nunca trabalhei com uma equipe tão competente, trabalhadora e dedicada como vocês. Sinto-me honrada de ter feito parte desse grupo.

Finalmente, gostaria de agradecer a todas as pessoas que contribuíram para a conclusão desse trabalho: Alexandre (absorção atômica), Orlando (ângulo de contato), Jéssica (AFM), Breno e Renata (MEV), Luzia e Késsia (FTIR), e muitos e tantos outros.

Muito obrigada!

RESUMO

Drenagem ácida de mina (DAM) é um efluente com baixo pH e altas concentrações de sulfato, metais e metaloides. O tratamento da DAM por processos de separação de membrana (PSM), especificamente nanofiltração (NF) e osmose inversa (OI), é de especial interesse uma vez que esses processos retêm de forma eficiente íons divalentes e produzem um permeado com qualidade suficiente para reuso industrial. A literatura indica a viabilidade técnica destes processos; no entanto, um estudo mais aprofundado é necessário, especialmente na otimização dos parâmetros operacionais, na análise da viabilidade econômica do processo, nas estratégias de limpeza química, e no envelhecimento da membrana. Assim, o objetivo desse estudo foi avaliar os principais parâmetros operacionais dos PSM, otimizar esses parâmetros, e estimar o custo capital e operacional do sistema (Capítulo 2). Foi objetivo desse estudo também estudar a incrustação da membrana durante o tratamento da DAM, avaliar o melhor procedimento para limpeza química da membrana, e o envelhecimento dessa membrana exposta ao concentrado da DAM e à solução de limpeza da membrana (Capítulo 3). Observou-se que apesar do pré-tratamento do efluente não diminuir a tendência à incrustação da membrana, ele melhora a qualidade do permeado final da NF. A NF apresentou maior potencial para esse tratamento que a OI, devido ao maior fluxo de permeado obtido e satisfatória eficiência de retenção de solutos. Dentre as membranas de NF, a NF90 apresentou a maior eficiência de retenção de solutos, e a NF270, o maior fluxo de permeado. O pH do efluente influenciou tanto a eficiência de retenção quanto a tendência à incrustação da membrana. A melhor combinação de tipo de membrana e pH foi a NF270 a pH 5,5. A taxa máxima de recuperação de água nessa condição foi 60%, quando se observou uma diminuição acentuada na eficiência de retenção e fluxo de permeado. Os custos capital e operacional estimados do sistema de UF-NF foram US$ 131.250,00, e 0,257 US$/$m^3$ de efluente. A DAM é composta principalmente por compostos inorgânicos dissolvidos, o que resulta em uma incrustação inorgânica rica em alumínio, arsênio, cálcio, cromo, níquel, potássio, e sódio. Dentre as soluções de limpeza estudadas, o melhor agente de limpeza foi o ácido clorídrico (HCl) com concentração de 0,20% m/m; essa concentração também proporcionou a menor exposição da membrana ao ácido. O envelhecimento da membrana pelo concentrado da DAM, e concentrado da DAM e periódica solução de HCl diminui a permeabilidade à água da membrana NF270. No entanto, a rejeição da membrana ao sulfato de magnésio e à glicose diminuiu menos de 10% em ambas as condições. Estes resultados sugerem que essa membrana é estável para essa aplicação.

Palavras-chave: Nanofiltração; osmose inversa; drenagem ácida de mina; reuso de água; pH do efluente; taxa de recuperação de água; limpeza química; envelhecimento da membrana.

ABSTRACT

Acid mine drainage (AMD) is an effluent characterized by low pH and high concentrations of sulfate, metals, and metalloids. AMD treatment by membrane separation processes (MSP), specifically nanofiltration (NF) and reverse osmosis (RO) is particularly interesting as these processes can retain divalent ions efficiently to produce high quality permeate for industrial reuse. The literature suggests the technical viability of these processes; however, further study is needed, in special on operational parameters optimization, on economic viability evaluation, on chemical cleaning strategies, and on membrane ageing. Therefore, the aim of this study was to evaluate the main operational conditions of the AMD treatment by MSP, optimize these parameters, and conduct a preliminary capital and operational cost evaluation (Chapter 2). Then, it aimed to evaluate the membrane fouling formed during AMD treatment, evaluate the best chemical cleaning procedure in this conditions, and the membrane ageing after prolonged exposure to AMD retentate and to the chemical cleaning solution (Chapter 3). The results showed that although effluent pretreatment had no considerable effect on the membrane-fouling tendency, it improved the final NF permeate quality. The NF showed higher potential for AMD treatment than RO, as it had higher permeate flux and satisfactory solutes retention efficiency. Among the NF membranes, the NF90 had the highest solutes retention efficiency, while the NF270 had the highest permeate flux. Effluent pH affected both the retention efficiency and the membrane-fouling tendency. The best combination of membrane type and feed pH was the NF270 at pH 5.5. The maximum water recovery rate at this condition was 60%, when a sharper decrease in retention efficiency and permeate flux was observed. The estimated capital and operational costs of the UF-NF system were US$ 131,250.00, and 0.257 US$/$m^3$ of effluent. The AMD is mainly comprised by dissolved inorganic compounds, which resulted in an inorganic fouling layer rich in aluminum, arsenic, calcium, chromium, nickel, potassium, and sodium. Among the evaluated cleaning solutions, the best cleaning agent was hydrochloric acid (HCl) at a concentration of 0.20% w/w; this concentration also provided the lowest membrane exposure to the acid. Membrane ageing caused by AMD retentate, and AMD retentate plus periodic HCl solution decreased the NF270 water permeability after 270 days by 49 and 45%, respectively. However, the membrane rejection to magnesium sulfate and glucose decreased less than 10% in both conditions. These results suggest that the NF270 membrane is stable during AMD treatment.

Keywords: Nanofiltration; reverse osmosis; acid mine drainage; water reuse; effluent pH; water recovery rate; chemical cleaning; membrane ageing.

SUMMARY

PUBLICATIONS

CONGRESS PUBLICATIONS:

AGUIAR, A.; ANDRADE, L.; PIRES, W.; AMARAL, M. Effect of Feed Ph in the Nanofiltration of Gold Acid Mine Drainage. 10th International Conference on Acid Rock Drainage & IMWA Annual Conference – 21 to 24 April 2015, Santiago, Chile.

AGUIAR, A.; ANDRADE, L.; PIRES, W.; AMARAL, M. Evaluation of Nanofiltration and Reverse Osmosis in the Treatment of Gold Acid Mine Drainage. 10th International Conference on Acid Rock Drainage & IMWA Annual Conference – 21 to 24 April 2015, Santiago, Chile.

AGUIAR, A.; ANDRADE, L.; PIRES, W.; AMARAL, M. Cleaning procedure for a NF membrane treating gold acid mine drainage. Euromembrane Conference – 7 to 10 September 2015, Aachen, Germany.

AGUIAR, A.; ANDRADE, L.; PIRES, W.; AMARAL, M. Nanofiltração Aplicada ao Tratamento de Drenagem Ácida de Mina de Ouro. 28º Congresso Brasileiro de Engenharia Sanitária e Ambiental – 4 to 8 October 2015, Rio de Janeiro, Brazil.

ARTICLES TO BE SUBMITTED:

A. O. AGUIAR, L. H. ANDRADE, B. C. RICCI, W. L. PIRES, G. A. MIRANDA, M. C. S. AMARAL. Gold acid mine drainage treatment by membrane separation processes: an evaluation of the main operational conditions

A. O. AGUIAR, L. H. ANDRADE, L. GROSSI, W. L. PIRES, M. C. S. AMARAL. Acid mine drainage treatment by nanofiltration: a study of membrane fouling, chemical cleaning, and membrane ageing

LIST OF FIGURES

LIST OF TABLES

LIST OF ABBREVIATIONS, ACRONYMS AND SYMBOLS

AMD – Acid Mine Drainage

MSP – Membrane Separation Processes

MF – Microfiltration

UF - Ultrafiltration

NF – Nanofiltration

RO – Reverse Osmosis

RR – Recovery Rate

CF – Concentration Factor

SEM/EDX – Scanning Electron Microscopy with Energy Dispersive X-ray Spectroscopy

AFM – Atomic Force Microscopy

ATR/FTIR – Attenuated Total Reflectance Fourier Transform Infrared Spectroscopy

1 CHAPTER

INTRODUCTION

1.1 Literature Review

1.1.1 Gold

Gold is known to mankind since ancient times. Its bright yellow color distinguishes it from other metals. Besides, gold's properties such as high corrosion resistance, malleability, ductility, high heat and electricity conductance and relative scarcity, made it a valuable element. Numerous civilizations before Christ were already able to use gold in jewelry and personal adornment due to natural gold deposits as nuggets and its ease of use (Schmid and Corain, 2003; Norgate and Haque, 2012).

Due to its high malleability, which can sometimes compromise the final product, in many cases gold is used in the form of alloys. The content of gold in an alloy is traditionally expressed in carats. The 24 carat gold has a purity degree of 99.99%, and is mainly used in the production of gold bars and coins for retail investment; the 18 carat gold has a purity degree of 75% (75% gold, 10 to 20% silver and 5 to 15% copper) and is extensively used in the production of jewelry in Europe and Brazil (DNPM, 2009).

However, the use of gold is not restricted to retail investment and jewelry. TABLE 1.1 presents world demand of gold by sector in the period 2005-2013. It can be observed that global gold demand also includes the electronic industry, which includes the production of computer boards, mobile phones and flat screen televisions. In 2013, this market accounted for 5.6% of total world demand (GFMS, 2014). Furthermore, there is a considerable demand of gold for dental purposes (primarily as dental prosthesis) and an increasing interest in its use for medical purposes. Functionalized gold nanoparticles, for example, are attracting scientific community interest due to their outstanding biocompatibility, excellent optical properties and great potential for biomedical applications. Functionalized gold nanoparticles have been studied especially in cancer treatment as sensors, in diagnosis and specific drugs carriers (Chen *et al.*, 2013).

TABLE 1.1 – World demand of gold in tons by sectors in the period 2005-2013

Demand	2005	2007	2009	2011	2013
Jewellery	2,721	2,425	1,817	2,029	2,361
Industry of electronics	286	322	275	320	279
Dental and medical	62	58	53	43	36
Other industrial uses	92	98	87	95	93
Retail investment (bars and coins)	412	442	825	1,569	1,778
Net official sector	- 663	- 484	- 34	457	409
TOTAL (tons)	2,910	2,861	3,023	4,513	4,956

Source: GFMS Gold Survey 2014, Thomson Reuters (GFMS, 2014).

Mining and mineral processing are activities of great economic importance in Brazil. Data from the Brazilian Institute of Geography and Statistics (IBGE) indicate that mineral extraction industry accounted for 4.1% of 2013 GDP (Gross Domestic Product) which corresponded to US$ 77.9 billion. Moreover, total exports of the jewelry productive chain reached US$ 3.2 billion in the same year (DNPM, 2014). In 2013, Brazil was the world's 11th largest gold producer, contributing a total of 79.9 tons as it is shown in TABLE 1.2 (GFMS, 2014).

TABLE 1.2 – Top gold mining countries in the years of 2012 and 2013

Rank		Country	Production (ton)	
2013	**2012**		**2013**	**2012**
1	1	China	438.2	413.1
2	2	Australia	266.1	251.4
3	4	Russia	248.8	229.7
4	3	United States	228.9	231.3
5	5	Peru	181.6	180.4
6	6	South Africa	174.2	177.3
7	7	Canada	133.1	108.0
8	9	Ghana	107.9	95.8
9	8	Mexico	103.8	102.8
10	10	Indonesia	99.2	89.0
11	**12**	**Brazil**	**79.9**	**67.3**
12	11	Uzbekistan	77.4	73.3
		Others	883.0	841.5
		Total	3,022.10	2,860.90

Source: GFMS Gold Survey 2014, Thomson Reuters (GFMS, 2014).

In 2013, four of the 26 Brazilian states accounted for 80% of the country's gold production: Minas Gerais (45.6%), Goiás (12.3%), Mato Grosso (11%), Pará (11%), Amapá (7.6), Bahia (7.4%), and Maranhão (3.6%) (DNPM, 2014).

Gold is one of the few metals found in the environment in its native state, rarely being combined with other elements. Native gold is the most common form of gold and possesses a gold content of 90% or more, moreover native gold is frequently accompanied by silver. Following native gold, the gold-silver tellurides are the most common gold minerals (Norgate and Haque, 2012). There are 19 known minerals to which gold may be combined, the most frequent minerals being the calaverite ($AuTe_2$) and sylvanite ($(Au,Ag)Te_2$) (DNPM, 2009).

Gold can be found in placer or lode deposits. Lode deposits are deposits of metalliferous ore which fills a fissure in a rock formation, or a vein of ore that is deposited between layers of rock. Placer deposits are those formed when stable minerals with high specific gravity are freed from their matrix by weathering processes and are slowly carried to stream beds, sand beds or crevices where they concentrate. Other minerals which can be found in placer deposits are platinum, zircon and various gemstones (Norgate and Haque, 2012).

From a metallurgical perspective, gold ores may be non-refractory (or free-milling) or refractory. Non-refractory minerals are easy to treat and gold recovery is obtained by gravity separating or direct cyanidation. Refractory gold ores are those where the gold is finely disseminated in the matrix of a sulfide host mineral, their treatment is more difficult and requires a pre-treatment prior to cyanidation. The pre-treatment might be an additional process such as roasting, bacterial oxidation or pressure oxidation. Over 90% of primary gold ores in Brazil are refractory ores (MME, 2009). Besides hindering the extraction of gold, the presence of sulfides may lead to the generation of acid mine drainages as will be explained later.

In conclusion, gold is a product of great importance to modern society and Brazil is one of the largest global producers of gold. Additionally, Minas Gerais leads national production holding almost 50% of total national production. As seen in many other industrial activities, mining and mineral processing are associated with many environmental impacts. Within this context, it is important to study measures to mitigate these impacts, especially in the state of Minas Gerais. These studies should promote a more sustainable gold production process.

1.1.2 Acid Mine Drainage

Mining operations have a direct impact on vegetation and wildlife, on surface and groundwater and on soil properties of the surrounding mining area. Open pit mines produce

huge soil movements which cause alterations on local topographic profile and create tailings deposits. It may also lead to soil erosion, noise pollution and air pollution due to the release of gas and particulates into the atmosphere. Underground mining, among other impacts, may result in damage to adjacent rocks by landslides and explosions and poor work conditions may pose health risks to operators.

Surface and groundwater can be affected by mining through disruption of hydrological pathways, possible increase in the rate of groundwater recharge, lowering of the water table, wastewater discharge, among others (Robles-Arenas *et al.*, 2006). The acid mine drainage (AMD) is an undesired wastewater generated at some mining sites which causes significant environmental problems. AMD occurrence has been reported in the extraction of gold, coal, copper, zinc and uranium (Trindade and Barbosa Filho, 2002). It has been recognized as one of the major environmental problems of mining activity not only due to its environmental impacts, but also due to the challenges of AMD control once initiated, the high volumes involved, the associated treatment costs, and the process perpetuity (Grande *et al.*, 2010).

AMD is characterized by its low pH and high concentration of sulfate (SO_4^{2-}); as well as high concentrations of metals (e.g. Fe, Cu, Pb, Zn, Cd, Hg, Ni, Co) and metalloids (especially As, but also Sb, Se) (Johnson and Hallberg, 2005; Robles-Arenas *et al.*, 2006; Sierra *et al.*, 2013). These pollutants are not biodegradable and tend to accumulate in living organisms, causing various diseases and disorders. Some environmental impacts associated with AMD include acidification of rivers and streams as well as leaching of toxic metals (Diao *et al.*, 2013).

Acid mine drainage (AMD) generation is initiated by the oxidation of metal sulfide (particularly pyrite (FeS_2), arsenopyrite (FeAsS) and pyrrhotite($Fe_{(1-x)}S$ with x = 0 to 0.17)) in mining waste, tailings and mine structures (such as pits and underground workings) of abandoned or active mines (Johnson and Hallberg, 2005; Anawar, 2013). As pyrite is the most reported cause of AMD, the oxidation of metal sulfide is often expressed in terms of pyrite oxidation. There are two main paths for pyrite oxidation. The first is through direct oxidation when exposed to oxygen and water, as expressed by EQUATION 1:

$$2FeS_2\ (s) + 7O_2 + 2H_2O \rightarrow 2Fe^{+2} + 4SO_4^{-2} + 4H^+ \qquad \text{(Eq. 1)}$$

The second is through reaction with ferric iron (Fe^{+3}), as expressed by EQUATION 2:

$$FeS_2(s) + 14Fe^{+3} + 8H_2O \rightarrow 15Fe^{+2} + 2SO_4^{-2} + 16H^+ \quad \text{(Eq. 2)}$$

Both pathways are fast (Costello, 2003; Anawar, 2013). The regeneration of ferric iron occurs when there is sufficient oxygen in the system as shown in EQUATION 3. Yet, this oxidation is known to be very slow and unstable at low pH except in the presence of microorganisms which may increase the rate of ferrous iron (Fe^{+2}) oxidation (Anawar, 2013).

$$4Fe^{+2} + O_2 + 4H^+ \rightarrow 4Fe^{+3} + 2H_2O \quad \text{(Eq. 3)}$$

Ferric iron can also precipitate as iron(III) hydroxide, the red-orange precipitate typically seen in AMD, as expressed by EQUATION 4:

$$2Fe^{+3} + 6H_2O \leftrightarrow 2Fe(OH)_3(s) + 6H^+ \quad \text{(Eq. 4)}$$

Sulfur- and iron-oxidizing microorganisms may catalyze EQUATIONS 1 and 3, increasing the production of sulfate and ferric iron. These microorganisms consist of the Bacteria and Archaea domains. In environments impacted by AMD the main bacterial genera reported were *Acidithiobacillus* (specially the specie *A. ferrooxidans*) and *Leptospirillum*, other genera reported were *Acidimicrobium*, *Acidisphaera*, *Acidobacterium*, *Acidocella*, *Acidiphilium*, *Alicyclobacillus*, *Ferrimicrobium*, *Frateuria*, *Sulfobacillus* and *Thiomonas*. The Archaea orders reported included the thermoplasmatales (specially the iron-oxidizing genus *Ferroplasm*), sulfolobales and methanomicrobiales (Mohapatra *et al.*, 2011).

According to Grande *et al.* (2010), AMD is an anthropogenic process as it results from the action of man. The oxidation of metal sulfides also occurs in undisturbed rocks, however at rates so slow that the water or the host rock is able to buffer the acid generated (Costello, 2003; Anawar, 2013). Due to mining activity and grain-size reduction, the surface area of metal sulfides increases and they become more prone to oxidation thus exceeding the buffering capabilities of the system.

There are basically two types of AMD remediation techniques: at-source control and migration control. At-source control techniques are aimed at preventing or minimizing the formation of AMD. These techniques are directed at the creation of chemical, biochemical and/or physical conditions that inhibit the oxidation of pyrite (Johnson and Hallberg, 2005;

Diao *et al.*, 2013). On the other hand, migration control techniques aim to remediate the AMD that has already been generated.

At-source control methods include selective handling and alkaline amendment, dry barriers, wet covers and biocides. Selective handling and alkaline amendment seeks to blend acid-producing and acid-consuming (such as carbonate) minerals to produce a benign composite. The accurate prediction of the amount of alkalinity needed in each situation has a significant cost and long-term liability implications. Moreover, the presence of alkalinity in the tailing and mining spoils does not ensure that the acidity will be neutralized as a direct contact between the infiltrating water and the alkalinity is needed (Barnhisel *et al.*, 2000). A variation of this method is the coating technology, or passivation. The coating is usually composed of phosphate or silicate composites and prevents the direct contact of pyrite with oxidizing agents (Diao *et al.*, 2013). Dry barriers and wet covers (underwater storage and flooding and sealing of abandoned deep mines) aim to retard the movement of oxygen and/or water into the acid-producing minerals, therefore minimizing AMD generation. Lastly, biocides have been applied in tailings and mining spoils to inhibit microbial activities, decreasing the rates of reactions expressed by EQUATIONS 2 and 3 (Johnson and Hallberg, 2005).

At first, at-source control methods may seem more attractive than traditional treatments as they can permanently solve AMD problems and do not require facilities for continued treatment after mine closure. However, these methods are unable to control 100% of the net-acidity produced on-site and migration control techniques would still be needed for the remaining AMD. Additionally, at-source control techniques for abandoned mines sites are generally unfeasible. This is mainly due to the absence of reliable mine maps and restricted access for the underground mines; and, for the surface mines, due to the huge volumes of tailings of unknown composition and expense related to rehandling and mixing these tailings (Barnhisel *et al.*, 2000).

Migration control techniques can be classified as passive or active system. Passive systems require relatively small amounts of resources and maintenance to sustain the process, while active systems require continuous addition of reagents. Both passive and active systems can rely on biological activities; however most of the biological remediation processes are passive systems. FIGURE 1.1 shows the main migration control technologies for AMD remediation (Costello, 2003; Johnson and Hallberg, 2005; Diao *et al.*, 2013; Sierra *et al.*, 2013).

FIGURE 1.1 – Migration control technologies for AMD remediation

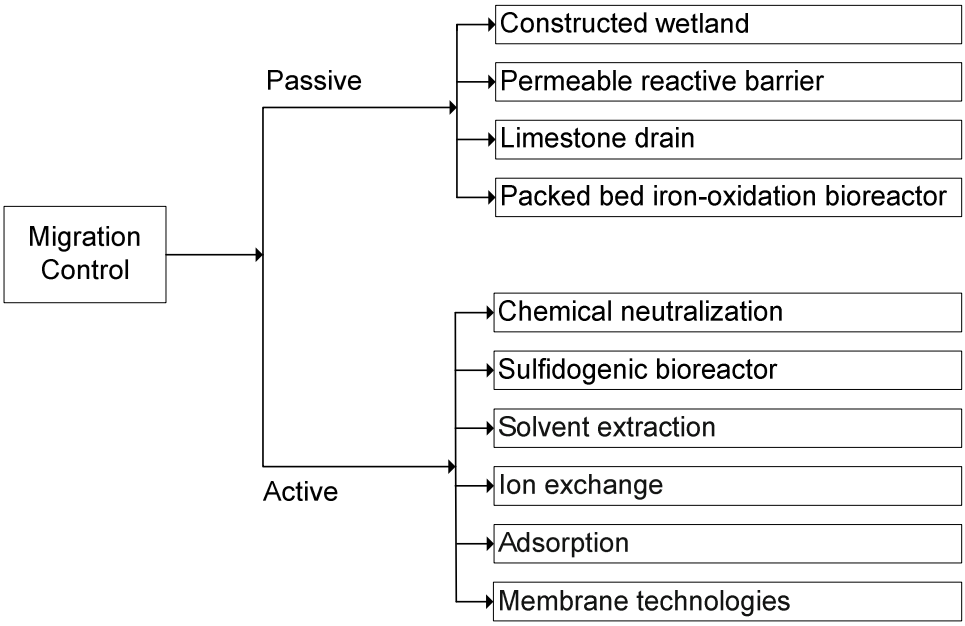

Among the migration control technologies, the most widespread is chemical neutralization. This process consists of continuously adding lime or other alkaline material in the AMD, increasing the effluent pH and precipitating many metals as hydroxides or carbonates. Although much used, this technology has the drawbacks of requiring large amounts of reagents and generating a secondary waste which must be properly disposed of. Besides, the precipitation of metals is not selective, thus hindering metal recovery (Sierra *et al.*, 2013).

Membrane separation processes (MSP) possess many advantages over traditional AMD treatments, such as adaptability to changes in flow characteristics, low operating times, modular design and ease of use. Furthermore, it produces a permeate with high quality which can be reused in the process thus reducing taxes over water catchment and effluent disposal. On the other hand, MSP have relatively high operational costs and membrane fouling may occur by salts precipitation, which increases the operational costs and decreases the process efficiency (Sierra *et al.*, 2013). Therefore, for this technology to be economically feasible in large scale in the treatment of gold AMD, the process must be thoroughly studied and optimized.

1.1.3 Membrane Separation Processes

Membrane separation processes (MSP) use a selective barrier (membrane) which under a driving force can promote the total or partial separation of the solution components. The feed solution is then divided into two streams: the fraction that crosses the membrane called the permeate; and the fraction which remains in the feed side called the retentate (Baker, 2012). FIGURE 1.2 shows a simplified diagram of a membrane separation process, here Q_f, Q_p and Q_r represents the feed, permeate and retentate flux, respectively; and C_f, C_p and C_r represents, respectively, the feed, permeate and retentate solution concentration of any solution component.

FIGURE 1.2 – Schematic diagram of a simplified membrane separation process

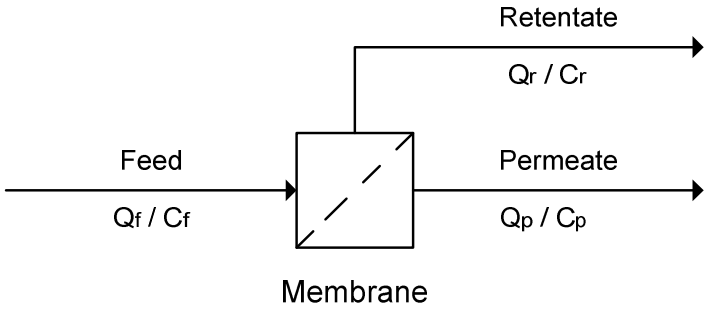

The pressure-driven MSP are the most well-established membrane technologies. They include: microfiltration (MF); ultrafiltration (UF); nanofiltration (NF); and reverse osmosis (RO). Classification of the pressure-driven membrane technologies are based on the membrane pore size and the size of particles and molecules retained by it. FIGURE 1.3 shows the pore size range of MF, UF, NF and RO membranes, and the size range of common constituents of aqueous solutions and streams (Li *et al.*, 2011). As can be seen in FIGURE 1.3, MF and UF processes use porous membranes with pore size, ranging from 100 to 5000 nm and from 10 to 100 nm, respectively (Jamaly *et al.*, 2014). They are low-pressure MSP and are used to remove microorganisms, and suspended and colloidal particles from the feed solution (Li *et al.*, 2011).

FIGURE 1.3 – Pore size range of pressure-driven MSP

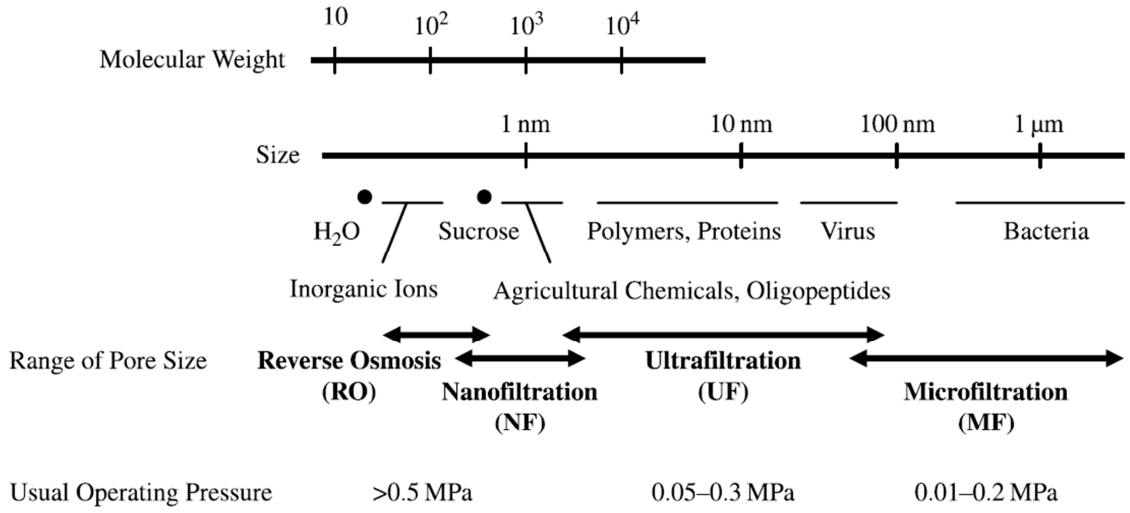

Source: Advanced membrane technology and applications (Li *et al.*, 2011).

RO membranes are dense non-porous membranes (Drioli and Giorno, 2009). The free volumes observed in these membranes are the spaces between the polymeric chains caused by thermal vibration of the polymer molecules (Baker, 2012). These membranes can separate solution components of low molecular weight, like monovalent inorganic ions (Jamaly *et al.*, 2014). The predominant transport mechanism through RO membranes follows the solution-diffusion model. In this model the solution components dissolve in the membrane material and then diffuse through the membrane. Thus, membrane selectivity is achieved due to differences in the solution components solubility in the membrane material, and differences in the solution components diffusion rate (Baker, 2012).

NF membranes are an intermediate between UF membranes and RO membranes (Hilal *et al.*, 2005; Baker, 2012). They have pore sizes ranging from 1-2 nm and can retain small molecules like divalent inorganic ions and sugars (Jamaly *et al.*, 2014). Permeation through NF membranes is a complex combination of molecular exclusion and charge interaction as well as on the solution-diffusion mechanism (Drioli and Giorno, 2009). Both NF and RO are of special interest in water and wastewater treatment, as they can retain macromolecules as well as dissolved inorganic ions.

The interest in MSP has increased expressively especially due to the need for more sustainable technologies, to the more restrictive regulations and directives, to the growing consumer demand for high-quality and safe products, to the increasing environmental concern, and to the confidence and acceptance of industry for advanced technologies.

Moreover, the increase in membrane units throughout the world has decreased the cost of membrane modules, thus making these processes more economically viable.

The literature presents few studies of AMD treatment with MSP. Al-Zoubi *et al.* (2010) studied the treatment of two synthetic AMD solutions with nanofiltration (NF99-Alfalaval and DK-GE-Osmonics) and reverse osmosis membranes (HR98PP- Alfalaval). Sierra *et al.* (2013) treated a mercury AMD using the NF-2540 membrane (FILMTEC™). Mullett *et al.* (2014) investigated the treatment of a cooper AMD with two NF membranes (NF 270-Dow and TS 80-TriSep). Although these studies point to the viability of this technology, they evaluate the effects of some operational parameters but do not attempt to optimize AMD treatment. The long-term viability of AMD treatment with MSP was even less studied. It depends on the membrane stability to the AMD solution, and to the chemical cleaning agent used to maintain membrane fouling controlled.

Therefore, this study aimed to evaluate some of the main operational parameters of MSP and optimize them. With this optimization, a more precise investment and cost estimate could then be conducted. Finally, membrane chemical cleaning was studied and membrane ageing during AMD treatment was investigated.

1.2 Justification

AMD is an effluent generated at some mining sites which has been recognized as one of the major environmental problems of mining activity. It is characterized by low pH and high concentrations of sulfate; as well as elevated concentrations of metals and metalloids. Mining and mineral processing are activities of great economic importance in Brazil and, in 2013, Brazil was the world's 11th largest gold producer; the state of Minas Gerais alone accounted for almost 50% of the national gold production. Therefore, the study in Minas Gerais of AMD mitigating technologies is well justified. MSP, specifically NF and RO are of special interest for AMD treatment since they can efficiently retain divalent ions like sulfate and metals. In addition, the high quality of the permeate obtained from both these processes indicates the possibility for water reuse in the industrial process. The literature indicates the technical viability of these processes; however, further study is needed, specifically on operational parameters optimization, economic viability and membrane ageing (due to contact with chemical cleaning solution and effluent).

1.3 Objectives

1.3.1 General Objective

The present study aims to investigate the use of nanofiltration and reverse osmosis in the treatment of gold acid mine drainage aiming at water production with high quality for industrial reuse.

1.3.2 Specific Objectives

The specific objectives are:

1. Investigate the influence of different pretreatments on the nanofiltration of AMD;
2. Evaluate different nanofiltration and reverse osmosis membranes, selecting the most suited for this application;
3. Study the influence of feed pH on the NF process and optimize this operational parameter;
4. Optimize water recovery rate aiming at higher permeate productivity and lower membrane-fouling tendency;
5. Conduct a preliminary investment and cost estimate of the optimized treatment system;
6. Evaluate membrane cleaning agents and optimize the cleaning solution concentration;
7. Investigate membrane fouling during AMD treatment;
8. Study the NF270 membrane ageing by AMD retentate and a combination of AMD retentate and cleaning solution.

1.4 Document Structure

This study consists of two parts. The first part, presented in Chapter 2, assess the influence of the main operational parameters of pressure-driven membrane separation processes on permeate flux and pollutants retention efficiencies. It comprises the specific objectives 1 to 5. The second part, presented in Chapter 3, investigates the membrane fouling by AMD and the chemical cleaning necessary to partially restore the fouled membrane. Moreover, membrane ageing by direct contact with the AMD retentate solution and chemical cleaning solution were evaluated. It comprises the specific objectives 6 to 8. Each chapter was presented in an independent manner, in an article format. Lastly, a summary of the experimental progress and suggestions for future research are presented in Chapter 4 and 5.

2 CHAPTER

GOLD ACID MINE DRAINAGE TREATMENT BY MEMBRANE SEPARATION PROCESSES: AN EVALUATION OF THE MAIN OPERATIONAL CONDITIONS

2.1 Introduction

Gold has high commercial value because of the unique properties and relative scarcity of this element. Gold mining and processing are important economic activities in Brazil, and, in 2013, the mineral extraction industry accounted for 4.1% of Brazil's GDP (Gross Domestic Product) (DNPM, 2014). More than 90% of the primary gold ore in Brazil is refractory ore (MME, 2009), which generally contains sulfide minerals. The oxidation of sulfide minerals in mining waste, tailings, and structures of active or abandoned mines can cause the formation of acid mine drainage (AMD). AMD is recognized as one of the most difficult environmental problems confronting mining companies; because of the ecological consequences of AMD, the difficulty of controlling it once it has started, the large volumes involved, the high associated treatment costs, and the perpetuity of the process (Grande *et al.*, 2010). AMD is characterized by low pH and high concentration of sulfate, as well as high concentrations of metals and metalloids (Johnson and Hallberg, 2005; Robles-Arenas *et al.*, 2006; Sierra *et al.*, 2013).

The mining industry, similar to many other industrial sectors, is positioning itself within the sustainability agenda, which encompasses concepts such as sustainability and sustainable development (Onn and Woodley, 2014). From a water usage perspective, this entails extracting natural resources at a rate lower than its natural replacement rate, and employing technological advancements to minimize and optimize the natural resources requirement. In this context, membrane separation processes (MSP) are the most promising technologies to reduce effluent discharge, and minimize water requirement through wastewater reclamation. MSP have high efficiency, reliability, ease of operation, high adaptability to changes in feed flow, low operation times, and modular design (Liu *et al.*, 2011). Both nanofiltration (NF) and reverse osmosis (RO) processes can retain salts and metals from the feed solution and, therefore, show high potential for AMD treatment aimed at water reuse (Fornarelli *et al.*, 2013). RO membranes are permeable to water but substantially impermeable to salts; therefore, they are suitable to separate ionic species, dissolved metals, and organic molecules of low molar mass (Baker, 2012). On the other hand, NF membranes are an intermediate between RO and ultrafiltration (UF) membranes. The NF membranes have higher permeate fluxes than RO membranes and can retain multivalent ions and dissolved molecules, with a molecular weight between 200 and 1,000 g/mol (Yu *et al.*, 2010).

However, NF and RO processes are highly susceptible to membrane fouling, which is caused by the deposition of organic and inorganic matter and/or the formation of biofilms on the membrane surface (Simon, Mcdonald, *et al.*, 2013). Although membrane fouling in MSP is inevitable, the rate and extent of fouling can be influenced by the feed characteristics, membrane properties, and operational conditions (Wei *et al.*, 2010). It is essential to control membrane fouling to ensure an economically feasible operation. Membrane fouling: increases the feed pressure requirement, which leads to higher energy consumption or lower system productivity; increases the chemical costs and reduces the membrane lifespan because of the increased cleaning frequency; increases the potential of damage to the membrane; and causes deterioration in the permeate quality because of reduced water permeability and higher concentration polarization (Ang *et al.*, 2011).

Feed characteristics play a significant role in determining foulant–membrane and foulant–foulant interactions, and, consequently, membrane-fouling tendency (Wei *et al.*, 2010). Effluent pretreatment can improve feed solution characteristics by removing some foulant compounds, such as colloidal impurities, inorganic precipitates, macromolecules, and biological contaminants, thereby reducing the fouling tendency of the membrane. Various technologies are available for effluent and water pretreatment and in the selection of the technology, one must consider the most expected membrane foulants. Inadequate feed pretreatment is the major cause for RO system failure/inefficiency (Chakravorty and Layson, 1997); therefore, the system should be well designed and operated. Moreover, variations in the feed quality have to be monitored, as they could be transferred to the NF or RO membranes (Pearce, 2008). Microfiltration (MF) and ultrafiltration (UF) are often used as effluent pretreatment for NF and RO systems. Because of the smaller pore size, MF and UF are more effective at removing fouling components and particulates than conventional pretreatments.

The membrane surface properties, such as hydrophobicity/hydrophilicity, surface roughness, and membrane charge density and charge polarity directly influence the fouling tendency of the membrane. The majority of commercial NF and RO membranes are made from polymers that have high thermal, chemical, and mechanical stability (Lalia *et al.*, 2013), and functional groups, such as -OH and -NH_2, can be added to the membrane surface to increase its hydrophilicity. The surface charge of NF and RO membranes improves the solutes rejection because of the electrostatic interactions between the charged solutes and the membrane.

Usually, commercial membranes are negatively charged to minimize the adsorption of negatively charged organic foulants and to increase salt rejection (Li *et al.*, 2011). The negative surface charge can be accomplished by adding functional groups, such as sulfonic and/or carboxylic acid groups, as these groups can deprotonate in the feed solution (Lalia *et al.*, 2013). Therefore, the surface properties of the membrane depend on the polymeric material of the membrane, the manufacturing process, and the added functional groups, as well as the conditions to which the membrane is exposed. The feed solution pH, for example, has a significant effect on the membrane charge and the distribution of solute species, as it can protonate and deprotonate the membrane functional groups and/or the molecules in the solution; and consequently, influences the process efficiency.

Finally, operational conditions, such as feed pressure, temperature, and feed flow rate, influence the convective transport of foulants toward the membrane surface (Wei *et al.*, 2010). Wang *et al.* (2005) have observed that higher operating pressures yielded higher initial permeate flux but faster decline in permeate flux with time, which is explained by the severer membrane fouling originated from foulants drag, denser foulant layers and consequent higher concentration polarization. They also studied crossflow velocity, and higher velocities lessened membrane fouling. This is explained by the back transport of solute to the bulk solution, consequently diminishing concentration polarization. However, one of the most important operational conditions for designing NF/RO systems is the water recovery rate. The water recovery rate (RR) is defined as the feed flow rate divided by the permeate flow rate. Consequently, higher RR implies higher system productivity and lower retentate production, which, consequently, influence the treatment capacity and the investment in equipment (Bi *et al.*, 2014). The water recovery rate is limited by an increase in the solute concentration of the feed solution. This increase leads to higher osmotic pressure, lower effective pressure, and higher fouling tendency because of the higher concentration polarization. Jamaly *et al.* (2014) pointed out that the water recovery rate had the strongest effect on both capital and operational costs.

Al-Zoubi *et al.* (2010) studied the treatment of two synthetic AMD solutions with nanofiltration (NF99-Alfalaval and DK-GE-Osmonics) and reverse osmosis membranes (HR98PP- Alfalaval). These authors evaluated the effects of pressure, temperature, and feed flow rate on pollutants rejection and permeate flux. The results showed that NF was more suitable for AMD treatment at low temperatures because of its higher permeate flux. The

rejection of heavy metal ions by nanofiltration (NF270-Dow membrane) was further investigated by Al-Rashdi *et al.* (2013) pertaining to the effects of feed pH, pressure, and metal concentration on cations rejection and permeate flux. These authors observed that metal rejection was higher at a feed pH below the membrane isoelectric point, attributable to the positive charge on the membrane surface. Tests were also carried out on non-synthetic AMD solutions. Sierra *et al.* (2013) treated mercury AMD by employing the NF-2540 (FILMTEC™) membrane. They studied the effects of pressure and volume reduction factor (feed concentration) and observed that the permeate flux was similar to the pure water flux up to a pressure of 10 bar, which suggests low concentration polarization. Moreover, the rejection of pollutants increased with the pressure and, at 10 bar, sulfate rejection was 88%. On the other hand, Mullett *et al.* (2014) investigated the treatment of copper AMD with two NF membranes (NF 270-Dow and TS 80-TriSep). They conducted feed pH and water recovery tests; however, only for the feed pH test with the NF 270 membrane used non-synthetic effluent. The results for this tests show that sulfur (S^{-2}) rejection increased with higher pH, while the rejection of cations (Ca^{+2}, Cu^{+2}, Mg^{+2}, and Mn^{+3}) decreased with higher pH. Moreover, all the reported rejections were higher than 88%.

Evidently, membrane separation processes showed high potential for AMD treatment, with high pollutants retention efficiencies. However, a thorough evaluation of AMD treatment in relation to all the main process characteristics was still needed. Therefore, the aim of this study was to evaluate gold AMD treatment relevant to feed pretreatment, membrane selection, pH adjustment, and maximum water recovery. With these conditions optimized, a more realistic cost assessment could be obtained.

2.2 Materials and Methods

2.2.1 Analytical Methods

Multi-element analyses of liquid samples were performed by ion chromatography (Dionex ICS-1000 ion chromatography, equipped with column type IonPac AS22 and IonPac CS12A). The other parameters analyzed were pH (pHmeter Qualxtron QX 1500), conductivity (Hanna conductivity meter HI 9835), turbidity (Hach 2100AN turbidimeter), and solid fractions. All analyses were performed in accordance with the *Standard Methods for the Examination of Water and Wastewater* (APHA, 2005).

2.2.2 Gold Acid Mine Drainage Characterization

AMD was collected at a gold mining company site in the state of Minas Gerais, Brazil. The company has two underground gold mines and an industrial processing plant. AMD was collected at one of the underground mines, at the fourth level below ground. The AMD flow rate at this industrial facility was 15 m^3/h. The AMD characteristics vary throughout the year, and the effluent properties of greatest interest to the present study are presented in TABLE 2.1.

TABLE 2.1 – AMD main characteristics

Characteristics	1st collection	2nd collection	3rd collection
pH	3.35	2.74	3.76
Color (uH)	30.1	31.1	268.4
Turbidity (UNT)	74	199	120
Total Organic Carbon (mg/L)	1.4	2.3	-
Conductivity (µS/cm)	2,841	2,744	2,573
Total Solids (mg/L)	2,409	2,926	3,102
Sulfate (mg/L)	984.5	1,406.1	1,959.5
Chloride (mg/L)	4.5	54.5	151.5
Calcium (mg/L)	282	323	284
Magnesium (mg/L)	125	97	226

Each batch of experiments used the same AMD collection sample to enable the comparison of the results.

2.2.3 Membrane Separation Processes

2.2.3.1 Microfiltration and Ultrafiltration

The microfiltration (MF) module was a submerged membrane module provided by Pam Membranas Seletivas Ltda., with a filtration area of 0.04 m^2, average pore diameter of 0.4 µm, and a polyetherimide-based polymer. MF occurred at a pressure of 0.7 bar, with up to 60% of water recovery.

The ultrafiltration (UF) module was a commercial submerged membrane (ZeeWeed) module, with a filtration area of 0.047 m^2, average pore diameter of 0.04 micrometers, and a PVDF-based polymer. UF occurred at 0.7 bar, with up to 60% of water recovery.

2.2.3.2 Nanofiltration and Reverse Osmosis

For the nanofiltration and reverse osmosis experiments, a bench-scale unit was used. This unit comprised the following: a supply tank, a pump, a valve for pressure adjustment, a rotameter, a manometer, a thermometer, and a stainless-steel membrane cell. The diameter of this membrane cell is 9.8 cm, providing a filtration area of 75 cm², and the diameter of the inlet channel is 0.64 cm. A feed spacer with approximate thickness of 1 mm was placed over the membrane to promote flow distribution. FIGURE 2.1 is a schematic of the NF/RO unit.

FIGURE 2.1 – Schematic of NF/RO unit

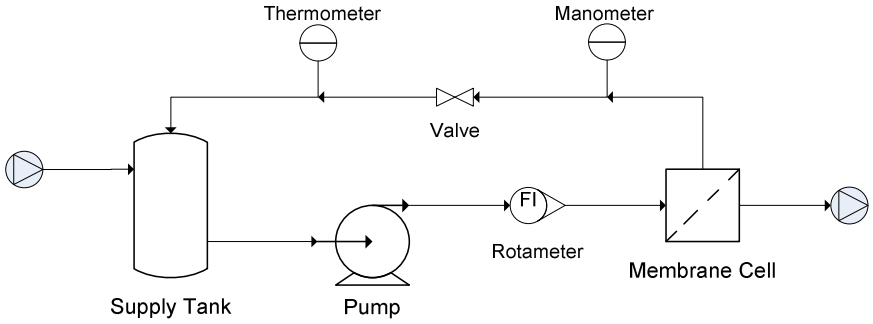

This unit used flat-sheet commercial membranes after they had been properly cut to fit the membrane cell. These membranes were first placed in an ultrasound bath with citric acid solution at pH 2.5, followed by an ultrasound bath with 0.1% NaOH solution, for 20 minutes each. This procedure aimed to remove possible residual components from the membrane surface. Subsequently, one clean membrane at a time was inserted onto the membrane cell and pre-compacted with distilled water at 10 bar, until permeate flux stabilization. Finally, the effluent filtration test was conducted at 10 bar, with a feed flow rate of 0.14 m^3/h, and the temperature at approximately 25 °C.

Permeate flux (J) was measured by collecting the volume of permeate by time in a measuring cylinder and dividing the result by the filtration area. The membrane water permeability (K) for each test was obtained from the linearization of the ratio of normalized permeate flux of pure water (J_N) by applied pressure (ΔP) at 10.0, 8.0, 6.0, and 4.0 bar. Flux normalization to 25 °C was accomplished by means of a correction factor related to the fluid viscosity, as shown in EQUATION 5:

$$J_N = \frac{\Delta V}{A \cdot \Delta t} \cdot \frac{\mu(T)}{\mu(25°C)} \quad \text{(Eq. 5)}$$

where $\Delta V/\Delta t$ is the permeate volume by time, A is the filtration area, J_N is the normalized permeate flux at 25 °C, $\mu(T)$ is the water viscosity at the process temperature, and $\mu(25\ °C)$ is the water temperature at 25 °C.

2.2.3.3 Resistance to filtration

According to the simplified resistance-in-series model, the total filtration resistance could be divided into intrinsic membrane resistance and fouling resistance. The intrinsic membrane resistance to filtration (R_M) was determined from EQUATION 6:

$$R_M = \frac{1}{K \cdot \mu(25°C)} \quad \text{(Eq. 6)}$$

The fouling resistance to filtration (R_F) was calculated based on the values of the normalized effluent permeate flux ($J_{N,E}$) obtained near the end of each experiment, as shown in EQUATION 7:

$$R_F = \frac{\Delta P - \sigma \cdot \Delta\pi}{\mu(25°C) \cdot J_{N,E}} - R_M \quad \text{(Eq. 7)}$$

where $(\Delta P - \sigma \cdot \Delta\pi)$ is the process effective pressure, i.e., applied pressure minus osmotic pressure, multiplied by the reflection coefficient (Noble and Stern, 1995). The reflection coefficient (σ) was estimated as the average molar retention, and the osmotic pressure difference was calculated using the van't Hoff equation (EQUATION 8):

$$\Delta\pi = \sum_{i=0}^{n} (C_r - C_p) \cdot R \cdot T \quad \text{(Eq. 8)}$$

where C_r and C_p are the concentrations of solute "i" on the retentate and permeate, respectively, R is the universal gas constant, and T is the temperature in Kelvin.

2.2.4 Evaluation of Effluent Pretreatment

The impact of feed pretreatment on nanofiltration was evaluated in terms of permeate quality, permeate flux, and fouling resistance. Three different feed solutions were used, namely, raw

effluent, effluent pre-filtered with qualitative filter paper (Fmaia - 8μm), and effluent pre-filtered by microfiltration. The AMD used on these experiments was from the 1st collection. Nanofiltration was carried out with the membrane NF90, supplied by Dow Filmtec (TABLE 2.2).

After the membrane was pre-compacted, nanofiltration with the three AMD feed solutions was carried out for two hours. The permeate flux and the temperature were measured every seven minutes. The final accumulated permeate was collected for analysis, while the retentate was continuously returned to the supply tank. Feed and permeate were analyzed for conductivity, total solids, and ion concentrations.

2.2.5 Nanofiltration and Reverse Osmosis Membranes Evaluation

The feed solution characteristics and the required permeate quality for reuse can directly influence the membrane selection for a given process. Three NF membranes and two RO membranes were compared for the treatment of gold AMD. The NF membranes analyzed were NF90, NF270, and MPF-34, while the RO membranes analyzed were TFC-HR and BW30. TABLE 2.2 shows the main characteristics of these membranes, as provided by the suppliers.

TABLE 2.2 – Membranes characteristics as provided by the suppliers

	Reverse Osmosis		Nanofiltration		
Characteristic	TFC-HR	BW30	MPF-34	NF90	NF270
Supplier	Koch Membrane	Dow Filmtec™	Koch Membrane	Dow Filmtec™	Dow Filmtec™
Membrane Material	Proprietary TFC® polyamide	Polyamide Thin-Film Composite	Proprietary SelRO™ composite	Polyamide Thin-Film Composite	Polyamide Thin-Film Composite
Maximum Operating Pressure (bar)	41	41	35	41	41
Maximum Operating Temperature (°C)	45	45	70	40	40
pH Range, Continuous Operation	4 - 11	2 - 11	0 - 14	2 - 11	2 - 11
NaCl Retention	99.55% [a]	99.5% [b]	35% [c]	85-95% [d]	-
$CaCl_2$ Retention	-	-	-	-	40-60% [e]
$MgSO_4$ Retention	-	-	-	> 97% [f]	> 97% [f]

[a] Test conditions: 2,000 mg/L NaCl at 15.5 bar applied pressure, 15% recovery, 25 °C, and pH 7.5.
[b] Test conditions: 2,000 ppm NaCl at 15.5 bar applied pressure, 15% recovery, and 25 °C.
[c] Test conditions: 5% NaCl at 30 bar, 30 °C.
[d] Test conditions: 2,000 ppm NaCl at 4.8 bar applied pressure, 15% recovery, and 25 °C.
[e] Test conditions: 500 ppm $CaCl_2$ at 4.8 bar applied pressure, 25 °C, and 15% recovery.
[f] Test conditions: 2,000 ppm $MgSO_4$ at 4.8 bar applied pressure, 25 °C, and 15% recovery.

The NF270, NF90, and BW30 Dow Filmtec™ membranes were selected to obtain a wide range of salt rejection values. The NF270 is a loose NF membrane, with low salt rejection; while the NF90 is a tight NF membrane, with moderate rejection; and the BW30 is a RO membrane, with high rejection, commonly used in the second pass of RO desalination (Tu *et al.*, 2011). On the other hand, the MPF-34 and TFC-HR Koch Membrane Systems® membranes were selected for stability over a wide range of pH (0–14) and high salt rejection, respectively. The TFC-HR membrane is a low-pressure RO membrane, typically used in the treatment of brackish water and in water reclamation (Fujioka *et al.*, 2012), whereas the MPF-34 membrane can be used for acid and caustic recovery because of its high pH resistance (Balanyà *et al.*, 2009).

AMD from the second collection was used for the membranes evaluation and MF was conducted as NF or RO pretreatment. The nanofiltration and reverse osmosis experiments were carried until a water recovery rate of 10% was achieved. The permeate flux, temperature, and the permeate accumulated volume were measured periodically. The final accumulated permeate was collected for analysis, while the retentate was continuously returned to the supply tank. Feed and permeate solutions were analyzed for conductivity, total solids, and ion concentrations.

2.2.6 Evaluation of Different Feed pH Values in Nanofiltration

The influence of feed pH on gold AMD nanofiltration was assessed. The nanofiltration membranes investigated were the NF90 and NF270, while the assessed feed pHs values were 3.2 (natural effluent pH), 4.2, 5.0, 5.5, and 6.0. The AMD used on these experiments was from the second collection.

Initially, the effluent pH was adjusted to the desired value with NaOH 5.0N solution, and, subsequently UF was conducted as NF pretreatment. Finally, NF was carried out for four hours. Permeate flux, temperature, and accumulated permeate volume were measured every 15 minutes. The final accumulated permeate was collected for analysis, while the retentate was continuously returned to the supply tank. Feed and permeate solutions were analyzed for conductivity, total solids, and ion concentrations.

2.2.7 Maximum Water Recovery Rate

The water recovery rate is defined as the ratio of feed flux (Q_f) to permeate flux (Q_p) (EQUATION 9). It is an important index for NF system design, since it affects the process capacity and the demand for investment in equipment.

$$RR = \frac{Q_p}{Q_f} \cdot 100\% \quad \text{(Eq. 9)}$$

The maximum water recovery rate for the treatment of gold AMD was experimentally determined. This experiment used AMD from the third collection. First, the pH of the AMD was adjusted to 5.5 and, subsequently, the effluent was pretreated with UF. Finally, a volume of 10 L of this pretreated effluent was nanofiltered. NF was carried out until a water recovery rate of 80% was obtained. The permeate was collected for analysis, while the retentate was continuously returned to the supply tank.

At every 100 mL of permeate obtained, the permeate flux and the temperature were measured; while at every 500 mL obtained, the conductivity and pH were measured; and at every 1,000 mL obtained, the ion concentrations were determined.

2.2.8 Preliminary Investment and Cost Estimate

A preliminary study was conducted to estimate the capital and operational expenses (CapEx and OpEx) of the optimized AMD treatment system. The following variables were considered: membrane unit cost, membrane replacement, alkalizing agents, chemical cleaning agents, energy consumption, and system maintenance.

The capital cost of the UF-NF membrane unit considered one filtration stage and a AMD volumetric flow of 15 m³/h, which is the capacity of the designed system (Q_{des}). To estimate the capital cost per cubic meter of effluent, the capital cost was annualized by means of the amortization factor, as presented in EQUATION 10 (Sethi and Wiesner, 2000):

$$A/P = \frac{i_c \cdot (1 + i_c)^{DL}}{(1 + i_c)^{DL} - 1} \quad \text{(Eq. 10)}$$

where (A/P) is the amortization factor, i_c is the investment rate (in 2015 was equal to 10% in Brazil), and DL is the design life of the plant. The UF-NF system design life was considered to be 15 years. The capital cost per cubic meter was obtained from EQUATION 11:

$$C_{cap/m^2} = \frac{C_{cap} \cdot A/P}{Q_{des}} \quad \text{(Eq. 11)}$$

where C_{cap/m^2} is the capital cost per cubic meter of effluent, C_{cap} is the system capital cost, and Q_{des} is the capacity of the designed system.

Membrane replacement costs considered an average membrane lifespan of 5 years. To determine the cost for membrane replacement, the required membrane area for UF and NF was determined. The recovery rate was set at 90% and 60% for ultrafiltration and nanofiltration respectively. An average permeate flux of 25 L/h.m² was considered for NF, and of 40 L/h.m² for UF. NF and UF membranes costs were 50.00 and 75.00 US dollars per square meter, respectively. These prices were provided by a large commercial membrane supplier.

The alkalizing agent used was NaOH. The volume of NaOH solution used to adjust the pH of the raw effluent was measured and used to estimate the neutralizing cost of the process. In this estimate, NaOH price was assumed as 425.00 US$/ton of NaOH[1]. In the cost estimation of the chemical cleaning agent, a cleaning frequency of once a week for one hour was assumed. The cleaning agent used was HCl solution at 0.2% w/w, which has an approximate price of 7.10 US$/L of HCl (37%)[2]. The volume of the cleaning solution considered the volume of the NF modules and the an estimated volume of the feed and return pipes.

The energy cost estimate comprised the UF power requirement and the NF feed pump requirement. The UF power requirement was estimated at 0.2 kWh/m^3 (Pearce, 2008). The NF feed pump requirement was obtained from EQUATIONS 12 and 13 (Sethi and Wiesner, 2000):

[1] Value available at: < http://www.icis.com/resources/news/2006/05/06/2013928/chemical-profile-caustic-soda/>. Accessed on: 13 October 2015.
[2] Value available at: < https://www.spectrumchemical.com>. Accessed on: 13 October 2015.

$$Q_f = \frac{J \cdot \mathrm{A}}{RR} \quad \text{(Eq. 12)}$$

$$E_f = \frac{\Delta P \cdot \mathrm{Q_f}}{\eta} \quad \text{(Eq. 13)}$$

where Q_f is the NF feed flow, E_f is the energy for feed pump, J is the average NF permeate flux (equals 25 L/h.m²), A is the total NF membrane area, RR is the water recovery rate (60%), ΔP is the applied pressure (10 bar), and η is the feed pump efficiency (considered as 70%). The energy tariff paid by this mining company in Brazil is 0.04 US$/kWh (considering an exchange rate of US$1 = R$0.25).

Maintenance costs were estimated at 5% per year of the initial investment cost (Shen *et al.*, 2014).

2.3 Results and Discussion

2.3.1 Evaluation of Effluent Pretreatment

Pretreatment is an important step in NF and RO operations, since the membrane will be less prone to fouling because of the removal of foulants components from the feed solution. Acid mine drainage (AMD) effluent with three different pretreatments were tested as NF feed solutions, namely, raw AMD, AMD pre-filtered with qualitative paper, and microfiltered AMD. The qualitative paper filter has a pore diameter of 8 μm, close to the pore diameter of industrial cartridge filters, which is approximately 5μm (Shahalam *et al.*, 2002).

The aim of this study was to evaluate the influence of suspended solids filtration in a later stage of nanofiltration. TABLE 2.3 shows the solids fraction obtained for the raw AMD sample. It is clear that, although the total solids (TS) content was extremely high, the total suspended solids (TSS) content was low, and represented only 1.5% of TS. Although small, this fraction will be totally retained by the NF/RO membrane, declining the permeate flux and reducing the membrane lifespan. Chakravorty and Layson (1997) highlighted the importance of robust pretreatment for RO, especially when the feed water was highly variable, when permeate quality characteristics were important, and when there was a shortage of skilled operators. All these conditions are met in AMD treatment aimed at water reuse.

TABLE 2.3 – AMD solids fraction

Total solids (mg/L)	Total fixed solids (mg/L)	Total volatile solids (mg/L)	Total suspended solids (mg/L)	Fixed suspended solids (mg/L)	Volatile suspended solids (mg/L)
2,409	1,845	564	36	27	9

As is apparent from TABLE 2.3 there is a high concentration of total fixed solids (TFS) compared with total volatile solids (TVS). The TVS is usually considered organic matter, although some organic matter will not volatize at high temperature (500 °C), while some inorganic matter will volatize (Tchobanoglous *et al.*, 2003). On the other hand, the TFS is mostly composed of inorganic matter and ions. Therefore, the main foulant anticipated in AMD treatment is scaling, and not biofouling. Scaling is formed by the crystallization and deposition of sparingly soluble inorganic salts. Various techniques can be applied to minimize scaling, such as pH adjustment, system design, and anti-scaling dosage (Karabelas *et al.*, 2014; Henthorne and Boysen, 2015). Because of the high concentrations of sulfate and calcium ions in AMD, calcium sulfate ($CaSO_4$) scaling is the most anticipated in AMD treatment. Jamaly *et al.* (2014) stressed the importance of anti-scaling evaluation and optimization prior to usage. In this study, anti-scaling was not used to enhance permeate recovery, since retentate treatment by precipitation (as $CaSO_4$ or $CaCO_3$) would be more difficult after an anti-scaling dosage. A detailed evaluation of AMD treatment with anti-scaling will be undertaken in future work.

TABLE 2.4 shows the concentration of the main pollutants in the permeate, and the system characteristics obtained during nanofiltration. The pollutant concentration was measured on the accumulated nanofiltration permeate (obtained with the NF90 membrane) for each feed pretreatment, while the observed retention efficiency (R_{obs}) was obtained from EQUATION 14:

$$R_{obs}(\%) = \frac{C_f - C_p}{C_f} \cdot 100\% \qquad \text{(Eq. 14)}$$

where C_f and C_p are the concentrations in the feed and permeate solutions for each solution component.

As is clear, all the retention efficiencies obtained were particularly high. Nevertheless, it was observed that using stronger pretreatment resulted in improved final permeate quality

(TABLE 2.4), probably because the process is more stable in this condition. As this treatment system aims to obtain a high quality permeate, suitable for reuse as process water, the retention of sulfate and calcium ions have to be optimized, as these ions can precipitate in pipes and equipment, resulting in damage. The increase in the retention efficiency of these ions is an advantage of using microfiltration prior to nanofiltration for the proposed treatment system. Chakravorty and Layson (1997) reported that microfiltration pretreatment was able to deal with high load variation in a desalination plant, while providing consistent water quality. On the other hand, media filters (such as the qualitative paper filter used in this study) could leak pollutants when the feed flow rate changed and/or became overloaded.

TABLE 2.4 – Concentration of the main pollutants on the permeate with the NF90 membrane, and system characteristics during nanofiltration

AMD Pretreatment	Characteristics	Raw AMD	Pre-filtered AMD	Microfiltered AMD
Permeate Concentration [Retention (%)]	Total Solids (mg/L)	495 (79.5)	482 (80.0)	293 (87.8)
	Calcium (mg/L)	93.9 (66.7)	82.3 (70.8)	42.8 (84.8)
	Magnesium (mg/L)	67.7 (45.9)	59.1 (52.8)	18.7 (85.0)
	Sulfate (mg/L)	7.2 (99.3)	6.7 (99.3)	5.2 (99.5)
	Chloride (mg/L)	1.4 (68.0)	1.1 (75.7)	1.2 (74.0)
System Characteristics	Reflection Coefficient (σ)	0.77	0.80	0.91
	$\Delta P_{effective}$ (bar)	9.67	9.64	9.53
	Average Permeate Flux by Water Flux (%)	87.1	79.1	79.1
	Water Permeability ($m^3/s.m^2.Pa$)	8.4×10^{-12}	1.3×10^{-11}	9.3×10^{-12}
	Membrane Resistance (m^{-1})	$1.3\times10^{+14}$	$8.5\times10^{+13}$	$1.2\times10^{+14}$
	Final Fouling Resistance (m^{-1})	$2.6\times10^{+13}$	$2.4\times10^{+13}$	$3.2\times10^{+13}$

TABLE 2.4 shows the values of the reflection coefficient and the process effective pressure for each AMD pretreatment. It is clear that the effective pressure of the experiment with microfiltered AMD was lower than that with raw AMD. This result was expected since the retention of pollutants in this condition was higher, increasing the reflection coefficient. Moreover, the osmotic pressure of the permeate (π_P) was lower, thereby increasing the osmotic pressure difference between the feed and the permeate solutions ($\Delta\pi = \pi_F - \pi_P$). As a result, we can conclude that for the same applied pressure (P), the process effective pressure (which is the driving force for filtration) is 1.5% lower with microfiltered AMD than with raw AMD.

The ratio of average effluent permeate flux by water flux was 87.1, 79.1, and 79.1, respectively, for the raw AMD, the pre-filtered AMD, and the microfiltered AMD (TABLE 2.4). In this case, effluent permeate flux by water flux was used to minimize the influences that variations in water permeability could have on the comparison of effluent permeate fluxes. The lower permeate flux with the microfiltered AMD can be partly explained by the lower effective pressure obtained in this condition. However, a complete investigation of the fouling mechanism is needed to fully explain the observed difference. The average permeate flux for the microfiltered AMD was 26.4 L/h.m^2. Sierra *et al.* (2013) obtained with the NF2540 membrane a permeate flux of approximately 45 L/h.m^2 for mercury AMD at an effective pressure of 10 bar and feed flow rate of 1,000 L/min. Besides the obvious difference in effluent solution and membrane characteristics, the increase in feed flow rate increases the shearing forces and decreases membrane fouling which could explain the higher permeate flux obtained.

The water permeability (K) of the NF90 membrane, membrane resistance to filtration (R_m), and fouling resistance (R_f) are indicated in TABLE 2.4 for each AMD pretreatment investigated. Water permeability was measured before effluent filtration, and its variability is a result of variations in the membrane characteristics, or in the effectiveness of membrane cleaning. From TABLE 2.4 it is clear that the final fouling resistances obtained after two hours of filtration for each pretreatment had the same order of magnitude, which suggests that the nanofiltration of raw, pre-filtered, and microfiltered AMD does not cause severe membrane fouling. The low fouling tendency is also corroborated by the low initial concentrations of fouling components, such as suspended solids and organic matter, in the raw effluent. However, even low concentrations of fouling components can directly increase the frequency of cleaning and maintenance of the membrane and, therefore, reduce the membrane lifespan. Moreover, the high variability of AMD throughout the year suggests the importance of pretreatment to prevent possible damage to or failure of the system. Additionally, microfiltration (or ultrafiltration) can ensure higher permeate flux, reduce fouling and chemical usage, and increase on-stream time (Pearce, 2008).

2.3.2 Evaluation of Nanofiltration and Reverse Osmosis Membranes

The retention of the total fixed solids (TFS) of the AMD can be accomplished by NF or RO processes. These two MSP can retain in a greater or lesser extent the dissolved ions in solution (main constituent of TFS) thus obtaining a permeate with high quality to be reused in

the industrial process. All five membranes used in this study are thin-film anisotropic composite membranes with a thin polyamide (PA) skin layer over a microporous support layer. Since the permeation rate is inversely proportional to the membrane thickness, a thinner membrane provides higher permeation rates. The membrane skin layer provides separation properties and permeation rates, while the microporous layer provides mechanical strength (Tu *et al.*, 2011; Baker, 2012).

TABLE 2.5 presents the water permeability, membrane resistance, fouling resistance at 10% of effluent recovery rate, and average permeate flux. As anticipated, the RO membranes tested (TFC-HR and BW30) showed permeate fluxes considerably lower than the NF membranes (MPF34, NF90, and NF270) during the filtration time. Among the NF membranes, the NF270 showed the highest permeate flux throughout the test. The average permeate flux of the NF270 membrane was 88.6 L/h.m^2, while the average permeate fluxes of the BW30 and TFC-HR RO membranes were 10.0 and 10.2 L/h.m^2, respectively, which confirmed the denser polymeric structure of these RO membranes. The NF270 membrane had a water permeability 44.1 and 58.8% higher than the other two NF membranes, namely, NF90 and MPF-34, respectively. These results are in accordance with the structure of these membranes and with the water permeability reported in other work (Balannec *et al.*, 2005; Balanyà *et al.*, 2009; Tu *et al.*, 2011).

TABLE 2.5 – Water permeability, membrane resistance, average permeate flux, and fouling resistance

Membrane	Water permeability ($m^3/s.m^2.Pa$)	Membrane resistance (m^{-1})	Average permeate flux ($L/h.m^2$)	Fouling resistance at 10% water recovery (m^{-1})
TFC-HR	3.4×10^{-12}	$3.3\times10^{+14}$	10.2±0.2	$4.1\times10^{+13}$
BW30	3.2×10^{-12}	$3.5\times10^{+14}$	10.0±0.3	$3.1\times10^{+13}$
MPF-34	1.4×10^{-11}	$8.1\times10^{+13}$	45.2±1.9	$4.8\times10^{+12}$
NF90	1.9×10^{-11}	$6.0\times10^{+13}$	55.7±3.0	$1.0\times10^{+13}$
NF270	3.4×10^{-11}	$3.3\times10^{+13}$	88.6±4.2	$1.1\times10^{+13}$

The required membrane area to treat the gold AMD flow is directly dependent on the average permeate fluxes obtained for each membrane. The evaluation of the required membrane area is crucial to the design of the NF/RO system, since it affects the capital investment (CapEx), as well as the operational and maintenance costs (OpEx). Because the NF has higher fluxes at lower applied pressure, it has been suggested as the preferable membrane separation process

for effluent treatment (Balannec *et al.*, 2005; Al-Zoubi *et al.*, 2010; Fornarelli *et al.*, 2013; Mullett *et al.*, 2014).

Moreover, higher fouling resistances were observed for the RO membranes than for the NF membranes (TABLE 2.5). The RO membranes tend to have higher concentration polarization resistances compared with the NF membranes, attributable to their higher rate of ionic rejection. In addition, these high rejections increases the fouling tendency of RO membranes, owing to an increase in ion concentration at the membrane surface that tends to precipitate. The membrane-fouling tendency in pressure-driven processes can also be influenced by the membrane surface properties, since membranes with smoother and/or more hydrophilic surfaces tend to have a lower fouling tendency (Wei *et al.*, 2013). Tu *et al.* (2011) reported a water contact angle of 54.6±3.0°, 50.9±4.9°, and 28.8±2.4° for the BW30, NF90, and NF270 membranes, respectively. Liu *et al.* (2011) reported a root-mean-squared roughness of 118.6±12.3nm and 72.8±9.5nm for the BW30 and NF90 membranes, respectively. Therefore, a lower fouling tendency was expected for the NF membranes compared with the RO membranes. Among the NF membranes, a lower water contact angle and lower surface roughness also increased water permeability and permeate flux.

TABLE 2.6 shows the main pollutant concentrations and the retention efficiency of the final accumulated permeate for each membrane. It is noteworthy the high retention efficiencies of these membranes. This results that all concentrations analyzed were lower than the concentrations obtained for the industry process water. Since RO membranes have denser polymeric structures, with a smaller molecular weight cut-off, higher retention efficiencies were expected for the TFC-HR and BW30 membranes. This was observed for the TFC-HR permeate, which had the lowest pollutant concentrations of all the parameters analyzed. However, the BW30 permeate had higher pollutant concentrations than the tested NF membranes had. The lower ionic rejection efficiencies of the BW30 membrane compared with the TFC-HR was also reported in the treatment of skimmed milk (Balannec *et al.*, 2005). Among the NF membranes, the NF90 showed the highest retention efficiency, which is in agreement with the structure of this membrane (Tu *et al.*, 2011). Moreover, the NF270 membrane not only provided a higher permeate flux than the MPF-34 but also had higher retention efficiencies. Bargeman *et al.* (2009) reported higher sulfate retention with the NF270 than with the MPF-34 in a vacuum-salt production plant, of, respectively, 98 and 89%.

The treated mother liquor in this plant contained 275–285 g/L of NaCl and 550–600 mmol/L of sulfate.

TABLE 2.6 – Main pollutants concentration and retention efficiency of NF/RO permeate for each membrane

Membrane	Permeate Concentration [Retention (%)]			
	Conductivity (µS/cm)	TS (mg/L)	Calcium (mg/L)	Sulfate (mg/L)
TFC-HR	78 (97.2)	38 (98.7)	< 2.5 (> 99.2)	2.2 (99.8%)
BW30	517 (81.2)	485 (83.4)	< 2.5 (> 99.2)	9.7 (99.3%)
MPF-34	442 (83.9)	295 (89.9)	10.3 (96.8)	4.1 (99.7%)
NF90	170 (93.8)	146 (95.0)	3.1 (99.0)	4.5 (99.7%)
NF270	379 (86.2)	207 (92.9)	8.8 (97.3)	2.6 (99.8%)
Process water [a]	710	1.374	104	304

[a] Process water quality

The selection of the most appropriate membrane for a given application should take into consideration both the quality of the final permeate and the average permeate flux, as these factors directly influence the capital and operational costs of the system. The low average permeate flux obtained for the TFC-HR membrane makes it cost-prohibitive for this application, especially since the NF membranes achieved satisfactory pollutant retention for water reuse. The BW30 membrane had low retention efficiency and low average permeate flux, and, consequently, was not suitable for AMD treatment. Among the NF membranes, the NF90 had the highest retention efficiency, while the NF270 had the highest average permeate flux; therefore, these two membranes were the most promising for AMD treatment.

2.3.3 Evaluation of Different Feed pH Values in Nanofiltration

The gold AMD studied has natural pH of approximately 3.2. The pH has to be neutralized for water reuse, as the process water has neutral pH. AMD neutralization can be performed before or after the UF and NF processes. Since the feed pH can directly influence the membrane properties and pollutants speciation, it can alter the nanofiltration performance. Therefore, a complete evaluation of the two most suitable membranes for AMD treatment at different feed pH was necessary. Membrane properties, such as membrane surface charge, isoelectric point, and pore size are the main pH-dependent properties (Carvalho *et al.*, 2011; Al-Rashdi *et al.*, 2013; Fornarelli *et al.*, 2013; Mullett *et al.*, 2014).

FIGURE 2.2 shows the ratio of permeate flux to pure water flux versus filtration time for the NF90 [FIGURE 2.2(a)] and the NF270 [FIGURE 2.2(b)] membranes. The permeate flux decreased continuously over time with both membranes because of an increase in concentration polarization, pore blocking, and initial fouling formation during filtration. TABLE 2.7 shows the values of membrane resistance and water permeability, as well as permeate flux by pure water flux, permeate flux, and fouling resistance at 40% RR. The different initial permeate fluxes led to different water recovery rates (RR) for each pH tested. Therefore, since permeate flux and fouling resistance are dependent on RR, these results were presented at a fixed RR of 40%.

FIGURE 2.2 – Permeate flux by pure water flux as a function of permeation time and feed pH for membranes a) NF90 and b) NF270

a)

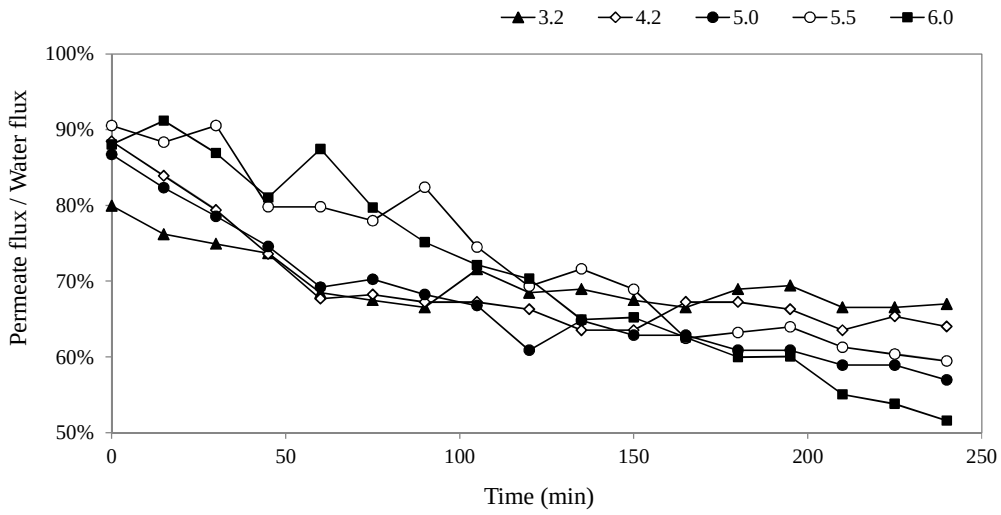

b)

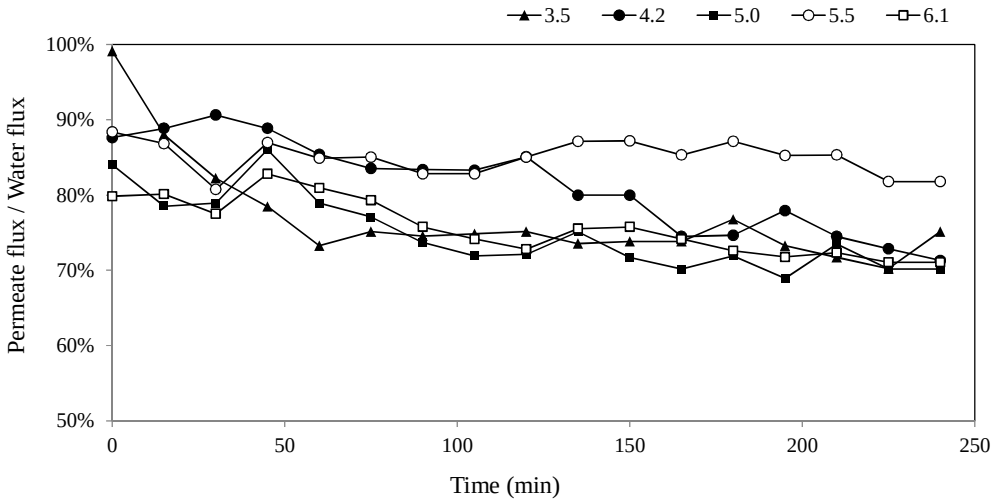

TABLE 2.7 – Membrane resistance, water permeability, permeate flux by pure water flux at 40% RR, permeate flux at 40% RR, and fouling resistance at 40% RR for the membranes NF90 and NF270

Membrane	pH	Membrane Resistance (m^{-1})	Water Permeability ($m^3/s.m^2.Pa$)	Permeate Flux by Water Flux (RR=40%) (%)	Permeate Flux (RR=40%) ($L/h.m^2$)	Fouling Resistance (RR=40%) (m^{-1})
NF90	**3.2**	$5.44\times10^{+13}$	2.06×10^{-11}	66.5%	49.5	$2.45\times10^{+13}$
	4.2	$5.34\times10^{+13}$	2.10×10^{-11}	64.4%	48.8	$2.63\times10^{+13}$
	5.0	$5.54\times10^{+13}$	2.03×10^{-11}	57.0%	41.6	$3.69\times10^{+13}$
	5.5	$5.20\times10^{+13}$	2.16×10^{-11}	64.0%	49.7	$2.48\times10^{+13}$
	6.0	$3.53\times10^{+13}$	3.18×10^{-11}	64.9%	74.4	$1.63\times10^{+13}$
NF270	**3.5**	$5.30\times10^{+13}$	2.12×10^{-11}	73.3%	55.9	$1.61\times10^{+13}$
	4.2	$4.80\times10^{+13}$	2.34×10^{-11}	74.5%	62.7	$1.22\times10^{+13}$
	5.0	$4.95\times10^{+13}$	2.27×10^{-11}	68.9%	56.3	$1.62\times10^{+13}$
	5.5	$5.35\times10^{+13}$	2.10×10^{-11}	85.3%	64.4	$3.50\times10^{+12}$
	6.1	$5.10\times10^{+13}$	2.20×10^{-11}	72.6%	57.5	$1.35\times10^{+13}$

The lower initial permeate flux by water flux for the NF90 membrane occurred at pH 3.2, the natural pH [FIGURE 2.2(a)] of AMD. However, flux decline during filtration at this pH was smaller, suggesting a lower tendency for membrane fouling. Moreover, the highest permeate flux at 40% RR was at pH 3.2, corresponding to 66.5% (TABLE 2.7). Therefore, this pH was the best operational condition for the NF90 membrane for gold AMD treatment. The initial permeate fluxes by water fluxes were higher at more neutral pHs (ph 5.5 and 6.0); but, with the rapid flux decline during filtration, the permeate flux at these pHs became smaller than that at pH 3.2. For example, at 40% RR, the permeate flux by water flux at pH 6.0 was 64.9% while at pH 3.2 was 66.5% (TABLE 2.7).

On the other hand, for the NF270 membrane [FIGURE 2.2(b)], pH 5.5 showed the smallest flux decline during filtration. At this pH, the permeate flux by water flux at 40% RR was 85.3% (TABLE 2.7). Additionally, the permeate fluxes by water fluxes for the NF270 membrane at all pHs were higher than those of the NF90 membrane. Hilal *et al.* (2005) reported higher pore size distribution for the NF270 membrane in comparison with the NF90, which, consequently, allowed for higher water permeability. Moreover, these authors reported higher surface roughness for the NF90 membrane. The surface roughness is responsible for the adhesive force, which results in a higher fouling tendency and increased permeate flux decay. Therefore, as anticipated, the NF270 membrane permeate flux by water flux at pH 5.5

and 40% RR (i.e., 64.4 L/h.m^2) was 23% higher than that of the NF90 membrane at pH 3.2 and 40% RR (i.e., 49.5 L/h.m^2).

The importance of dividing permeate flux by water flux in comparing the results of TABLE 2.7 has to be emphasized. If permeate fluxes (in L/h.m²) were analyzed separately, it would indicate that the NF90 membrane at pH 6.0 was preferable for AMD treatment. However, its higher permeate flux is a direct result of the lower membrane resistance and higher water flux. Commercial membranes such as the NF90 and NF270 are not homogeneous; therefore, the water permeability of a specific part of the membrane used in a one test could differ from that of another part of the membrane used in a subsequent test.

TABLE 2.8 shows the sulfate, calcium, and magnesium concentrations and retention efficiencies of the NF90 and NF270 accumulated permeates for each pH tested. Higher ionic retentions were observed with the NF270 membrane compared with the NF90 membrane, even though the NF90 is a tighter NF membrane than the NF270 and, therefore, should have higher ionic rejections. The observed higher salt rejection could occur for more permeable membranes because of the higher water flux, which could counterbalance the higher salt permeation and provide a higher net rejection (Ghosh *et al.*, 2008).

TABLE 2.8 – Main ionic concentrations and retention efficiencies of the NF90 and NF270 accumulated permeates at each feed pH

pH	Sulfate (mg/L) [Retention (%)]		Calcium (mg/L) [Retention (%)]		Magnesium (mg/L) [Retention (%)]	
	NF90	NF270	NF90	NF270	NF90	NF270
3.2	548.6 (61.0)	-	133.2 (58.8)	-	98.3 (-)	-
3.5	-	451.0 (75.6)	-	102.3 (68.3)	-	85.1 (12.5)
4.2	532.2 (62.2)	257.5 (86.1)	110.3 (65.9)	80.0 (75.2)	93.1 (4.3)	62.8 (35.5)
5.0	679.4 (51.7)	230.0 (87.5)	45.2 (86.0)	42.7 (86.8)	28.0 (71.2)	25.4 (73.9)
5.5	518.3 (63.2)	256.5 (86.1)	62.3 (80.7)	22.2 (93.1)	45.1 (53.6)	5.0 (94.9)
6.0	452.9 (67.8)	-	79.6 (75.4)	-	62.4 (35.9)	-
6.1	-	264.6 (85.7)	-	36.3 (88.8)	-	19.1 (80.4)

The exclusion of charged particles by nanofiltration is governed by a sum of convective and diffusive effects, steric hindrance, and electrostatic repulsion; therefore, the membrane surface charge plays an important role in the retention of AMD pollutants. The membrane surface charge can be characterized by the zeta potential, which is usually evaluated by streaming

potential measurements with electrolyte solutions. The solution pH that leads to a neutral membrane charge is defined as the membrane isoelectric point (IEP). At pH vaues lower than the IEP, the membrane is positively charged, while, at pH values higher than the IEP, it is negatively charged (Li *et al.*, 2011). The literature reports numerous zeta potential measurements of the NF90 and NF270 membranes with different electrolyte solutions. TABLE 2.9 shows a summary of these results. The average IEP values obtained for the NF270 and NF90 membranes from the literature were 3.0 and 5.3, respectively. The variability of the reported IEP values is mostly related to differences in the chemical solutions used in each test. In addition, the solution pH and the hardness cations also have a significant effect on the membrane charge (Teixeira *et al.*, 2005).

TABLE 2.9 – Reported NF90 and NF270 membranes zeta potential

Membrane	Author	pH Range	Electrolyte Solution	IEP
NF90	Carvalho *et al.* (2011)	4-8	0.1 mMKCl	5.7
	Tu *et al.* (2011)	2.5-10.5	10 mMKCl	4.8
	Do *et al.* (2012)	3-9	10 mMNaCl	5.5
NF270	Tanninen *et al.* (2004)	-	1 mMKCl	3.3
	Dalwani *et al.* (2011)	2-11	5 mMKCl	3.2
	Tu *et al.* (2011)	2.5-10.5	10 mMKCl	2.7
	Do *et al.* (2012)	3-9	10 mMNaCl	3.1
	Simon, Price, *et al.* (2013)	2.5-10	1 mMKCl	2.8

At the isoelectric point, the membrane charge is zero and salt rejection is expected to be minimal because of a lack of electrostatic repulsion (Mullett *et al.*, 2014). This explains the minimal sulfate retentions observed in the NF90 and NF270 membranes at pH 5.0 (i.e., 51.7%) and pH 3.5 (i.e., 75.6%) (TABLE 2.8), both of which were quite close to the average IEP reported in the literature. The lower sulfate retention with the NF90 membrane can also be better explained in terms of the membrane surface charge. Ionic separation by electrostatic repulsion is based on the Donnan exclusion mechanism. According to this mechanism, co-ions (ions with the same charge as the membrane) are repelled by the membrane surface and, subsequently, counter-ions are retained by the membrane to maintain the electroneutrality of the solution (Teixeira *et al.*, 2005). At pH higher than 3.5, the NF270 membrane had a negative surface charge and, consequently, selectively repelled anions and retained cations. Since the sulfate (SO_4^{-2}) is a divalent anion, it is more strongly repelled by the NF270 membrane. On the other hand, the NF90 membrane was positively charged at pH lower than

5.0. Consequently, the sulfate was retained to maintain the electroneutrality of the solution. However, this process is not as selective as the electrostatic repulsion. At pH higher than 5.0, the NF90 membrane increased the sulfate retention and higher pH (and therefore higher negative surface charge) led to higher sulfate retention.

In conclusion, the NF270 membrane showed better potential for the treatment of gold AMD compared with the NF90 membrane. The NF270 membrane provided a higher permeate flux by water flux at a water recovery rate (RR) of 40%, lower initial membrane investment, and higher ionic retentions. Among the pH values tested with the NF270 membrane, pH 5.0 had the highest sulfate retention (87.5%) but the lowest permeate flux by water flux at 40% RR (68.9%). On the other hand, pH 4.2 and pH 5.5 showed median values of sulfate retention (86.1% in both instances). Furthermore, at pH 5.5, the NF270 showed the highest calcium and magnesium retentions (respectively, 93.1% and 94.9%) and the highest permeate flux by water flux at 40% RR (85.3%). It follows that the NF270 membrane at pH 5.5 had the highest potential for gold AMD treatment.

2.3.4 Maximum Water Recovery Rate

The water recovery rate is an important index for designing water treatment plants by pressure-driven membrane separation processes, since it directly influences treatment capacity, equipment investment, membrane-fouling tendency, and operational costs. An increase in the recovery rate leads to increased feed solution concentration over filtration time and higher concentration polarization, which reduce the retention efficiency.

The permeate concentration and retention efficiency of the main dissolved ions as a function of the water recovery rate are presented in TABLE 2.10. FIGURE 2.3 shows the permeate conductivity and conductivity retention by the water recovery rate. The values presented in TABLE 2.10 and FIGURE 2.3 are the concentration and conductivity obtained after every 1.000 and 500 mL of permeate, respectively; after the measurement, the permeate sample was stored and a new sample started (at a higher recovery rate). Therefore, these values do not reflect the quality of the final accumulated permeate, but the quality of the effluent generated at that specific recovery rate. An increasing trend can be observed in the permeation of pollutants with the increase in the recovery rate. Moreover, as can be seen in TABLE 2.10, the permeate quality obtained up to a recovery rate of 60% was higher than the quality of the process water used by this mining company (TABLE 2.6). This finding suggests the viability

of permeate reuse in the industrial process. At RR higher than 60%, the magnesium concentration in the permeate was slightly superior to that of the process water. However, this difference does not diminish the potential to reuse the permeate, since the magnesium concentration was still below the critical values for water. The continuous decline in the quality of the permeate is also clear from FIGURE 2.3, with the increase in permeate conductivity with recovery rate. A sharp decline in conductivity retention efficiency was observed at 60% RR. At 60% RR, the conductivity was 545 µS/cm, which increased to 1628 µS/cm at 70% RR. Bargeman *et al.* (2009) treated sulfate waste in a vacuum-salt production plant for 500 h at CF = 1.2–1.4 and reported a stable sulfate retention between 97 and 90%.

TABLE 2.10 – Main pollutants concentration and retention efficiency of the AMD permeate with the NF270 membrane at ph 5.5, at every 10% of water recovery rate

Recovery Rate (%)	Permeate Concentration [Retention (%)]			
	Calcium (mg/L)	Magnesium (mg/L)	Sulfate (mg/L)	Chloride (mg/L)
10	3.5 (98.8)	4.2 (98.2)	64.2 (96.7)	1.9 (98.8)
20	3.7 (98.7)	3.0 (98.7)	64.8 (96.7)	1.6 (98.9)
30	5.3 (98.1)	4.6 (98.0)	91.4 (95.3)	3.3 (97.8)
40	6.9 (97.6)	8.1 (96.4)	119.5 (93.9)	3.2 (97.9)
50	15.1 (94.7)	10.7 (95.3)	192.4 (90.2)	3.1 (97.9)
60	13.3 (95.3)	10.8 (95.2)	262.1 (86.6)	4.4 (97.1)
70	20.1 (92.9)	13.0 (94.3)	273.1 (86.1)	4.8 (96.8)
80	27.7 (90.2)	14.4 (93.6)	301.6 (84.6)	6.0 (96.1)

FIGURE 2.3 – Conductivity and conductivity retention efficiency of the AMD permeate with the NF270 membrane as a function of water recovery rate

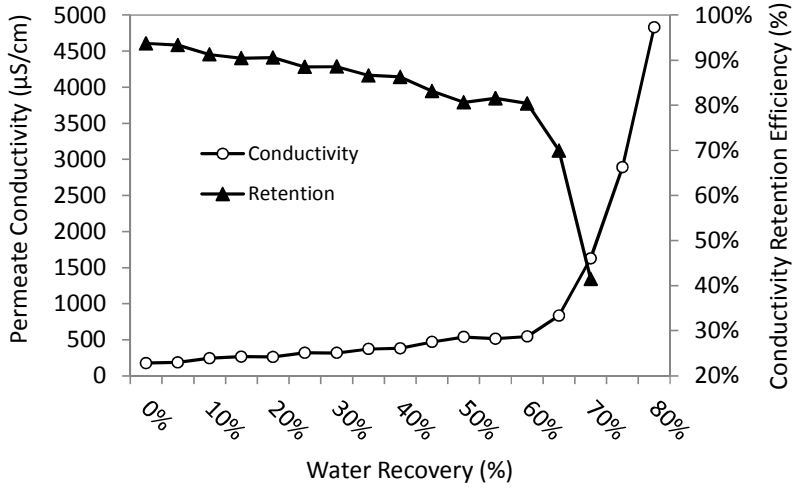

The concentration factor (CF) is a widely used parameter in RO systems to determine the feed solution concentration over filtration time. Since salt permeation in RO is close to zero, the CF can be simply calculated from the water recovery rate. However, salt permeation in NF systems is not zero, and an observed salt retention factor must be considered in the calculation of CF, as shown in EQUATION 15 (Bi *et al.*, 2014):

$$CF = \frac{C_r}{C_f} = \frac{1 - RR \cdot (1 - R_{obs})}{1 - RR} \quad \text{(Eq. 15)}$$

where C_r and C_f are the molar concentrations in the retentate and the feed solutions, respectively, and R_{obs} is the observed molar salt retention. The observed molar salt retention (R_{obs}) is the total accumulated permeate retention of the main ions at a specific recovery rate, which was calculated by the arithmetic mean of the permeate molar retentions before each RR. FIGURE 2.4 shows the relation between RR and CF, and the observed salt retention (R_{obs}) by CF. Water recovery rate and concentration factor are both used to reflect the concentration degree of the feed solution. The decrease in R_{obs} with CF was expected because of the higher salt concentration at the membrane surface (C_m) and concentration polarization.

FIGURE 2.4 – Observed salt retention (R_{obs}) and recovery rate (RR) by concentration factor (CF)

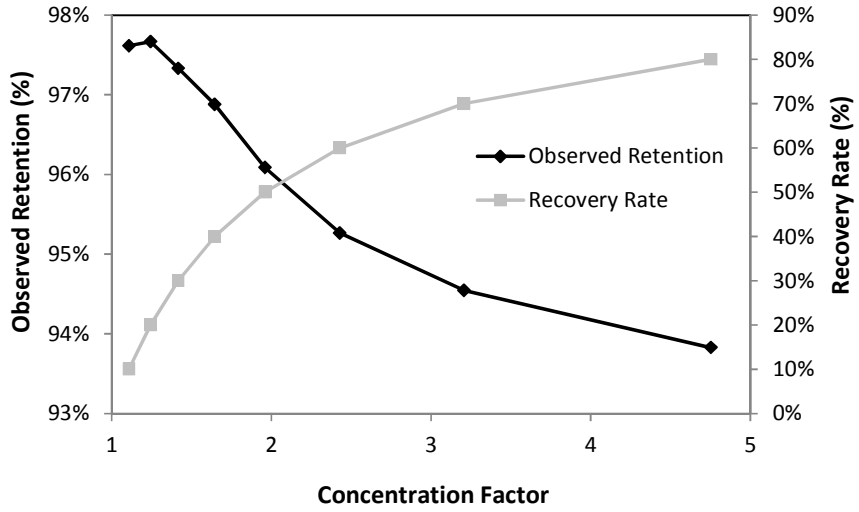

The salt concentration at the membrane surface (C_m) can be obtained by EQUATION 16 (Noble and Stern, 1995):

$$\frac{C_m - C_p}{C_r - C_p} = \exp\left(\frac{J}{k}\right) \quad \text{(Eq. 16)}$$

where C_r and C_p are the molar concentrations in the retentate and permeate, respectively, J is the permeate flux (in $m^3/h.m^2$), and k is the mass transfer coefficient. The mass transfer coefficient was calculated as demonstrated by Ricci *et al.* (2015), and its numerical value was 6.56×10^{-5} and 5.46×10^{-5}, respectively for SO_4^{-2} and Ca^{+2}. With C_m, the membrane real rejection (R_{real}) can be determined by EQUATION 17:

$$R_{real} = \left(1 - \frac{C_p}{C_m}\right) \cdot 100\% \quad \text{(Eq. 17)}$$

The molar concentration at the membrane surface (C_m) and the real rejection (R_{real}) for calcium and sulfate ions are shown in FIGURE 2.5 as a function of the recovery rate (RR). The increase in RR led to an increase in C_m; however, R_{real} was almost constant throughout the filtration time. This indicates that the membrane selectivity was preserved during AMD treatment.

FIGURE 2.5 – C_m and R_{real} values for calcium and sulfate at different RR

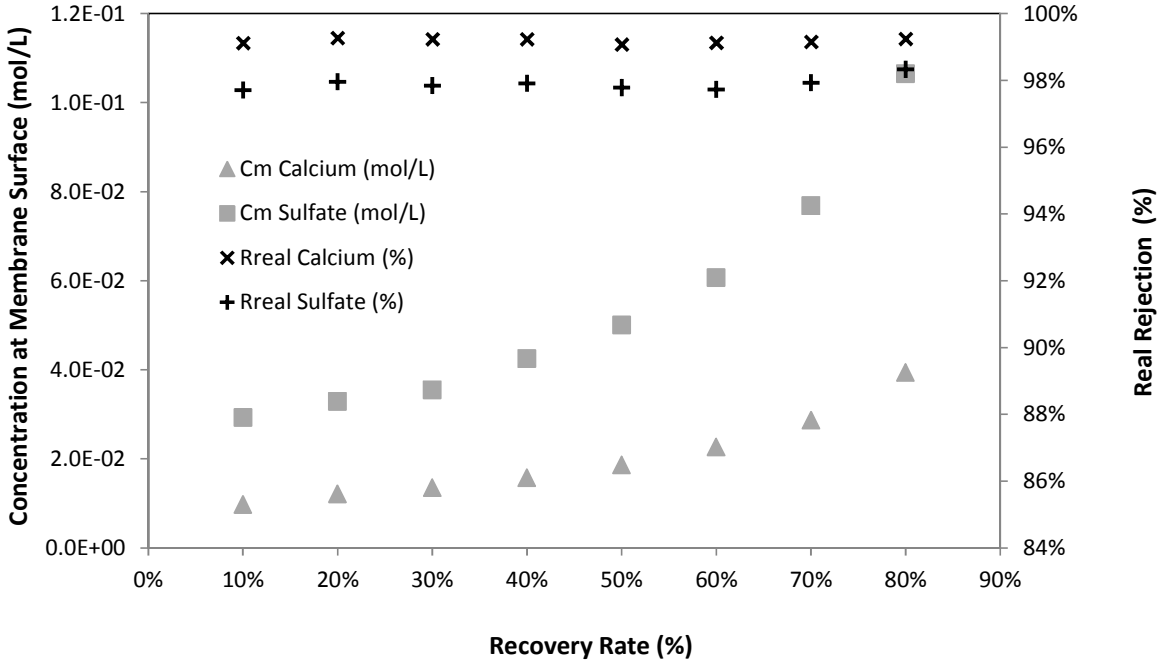

To conclude, $CaSO_4$ supersaturation degree was calculated, as shown in EQUATION 18 (Ricci *et al.*, 2015):

$$S = \left[\frac{IP}{K_{ps}{}'}\right]^{\frac{1}{2}} \quad \text{(Eq. 18)}$$

where $K'_{sp}$is the solubility product under operational conditions, and IP is the product of the molar concentration of calcium and sulfate ions.

$$K'_{sp} = \frac{K_{sp}}{\gamma_{Ca^{2+}}\gamma_{SO_4{}^{2-}}} \quad \text{(Eq. 19)}$$

where K_{sp} is the calcium sulfate solubility product at 25 °C and at ionic strength equal to zero, and $\gamma_{Ca^{2+}}$ and $\gamma_{SO_4{}^{2-}}$ are the activity coefficients of calcium and sulfate ions, respectively, predicted by Davies equation. Because of concentration polarization, the calcium and sulfate concentrations at the bulk of the solution (C_f or C_r) and at the membrane surface (C_m) differed; consequently, the supersaturation degree was calculated separately for these two conditions. TABLE 2.11 shows the values of supersaturation degree (S) for water recovery rates up to 80%. The solution was supersaturated when the supersaturation degree was higher than unity. It is clear that the feed solution (at RR = 0%) was not supersaturated ($S_b < 1$), but, at 10% RR, the retentate bulk solution was already supersaturated (S_b = 1.03). The supersaturation degree in the bulk solution continuously increased with RR because of the increased ionic concentration in the solution. Moreover, for all RR values, the supersaturation degree (S_m) of the membrane surface was higher than the supersaturation degree (S_b) of the bulk solution, because of the concentration polarization. When the solubility limit for mineral salt is exceeded, a potential membrane scaling problem could occur and antiscaling is recommended for the feed solution (Bader, 2007; Gabelich *et al.*, 2007). However, in the entire experiment, $CaSO_4$ precipitation was not observed and the industry guidelines recommend an upper operating limit of supersaturation below 2.3 for $CaSO_4$ (TAB, 2008). Since the supersaturation degree at the membrane surface was lower than 2.3 for RR lower than 60%, antiscaling was not mandatory. However, it could still increase maximum water recovery and decrease the fouling tendency.

TABLE 2.11 – Supersaturation degree in the bulk of the solution (S_b) and at the membrane surface (S_m) at different recovery rates

Recovery Rate (%)	0%	10%	20%	30%	40%	50%	60%	70%	80%
S_b	0.96	1.03	1.11	1.19	1.34	1.51	1.74	2.12	2.85
S_m	-	1.37	1.48	1.57	1.75	1.95	2.22	2.58	3.24

The water recovery rate (RR) is mostly restricted by scaling fouling formation and osmotic pressure increase (Bi *et al.*, 2014). FIGURE 2.6 shows the permeate flux and process effective pressure versus water recovery rate (RR). The process effective pressure ($\Delta P_{effective}$) continuously decreased because of the increase in ionic concentration of the feed solution, which, consequently, increased the osmotic pressure (π_f) of the feed solution and the osmotic pressure differential ($\Delta\pi$). It is clear from FIGURE 2.6 that up to a RR value of approximately 60%, permeate flux decay followed the effective pressure decay. This shows there was no severe scaling fouling on the membrane surface. Moreover, the decrease in the process driving force ($\Delta P_{effective}$) was the sole reason for the variation of permeate flux up to 60% RR. However, after 60% RR, the permeate flux decay was sharper than the effective pressure decay. This implies that the decrease in the driving force alone did not explain the variation in permeate flux; therefore, we had to consider that membrane fouling was taking place. The initial normalized permeate flux was 61.2 L/h.m^2, decreasing to 52.3 L/h.m^2 at 60% recovery, and reaching 27.7 L/h.m^2 at the end of the experiment (RR = 80%).

FIGURE 2.6 – Permeate flux, natural logarithm of fouling resistance, and process effective pressure as a function of water recovery rate

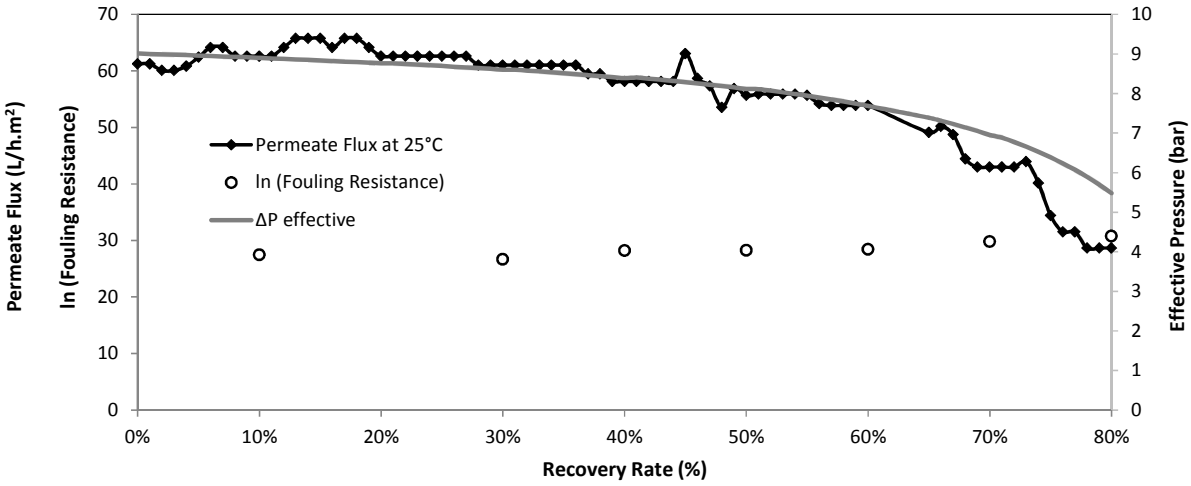

FIGURE 2.6 shows the natural logarithm of fouling resistance and membrane resistance versus the water recovery rate. The fouling resistance for 20% RR is not shown here, as it provided a negative value. The fouling resistance was calculated as the total resistance minus the membrane resistance (EQUATION 7); therefore, a negative value simply indicated the proximity of the membrane resistance to the total resistance, and was within the experimental error. After 60% RR, the fouling resistance increased slightly, which aided understanding the sharper decrease in permeate flux (FIGURE 2.6) after this recovery rate.

In conclusion, the maximum water recovery rate obtained for a single NF step in the treatment of gold AMD with the NF270 membrane was 60%. Above this RR, the permeate flux decay would be sharper than the effective pressure decay, membrane fouling would be more severe, and permeate quality would decline.

2.3.5 Preliminary Investment and Cost Estimate

TABLE 2.12 shows a summary of the main capital and operational expenses (CapEx and OpEx) of the NF treatment system. The CapEx of the UF-NF unit was US$131,250.00. The required UF and NF membrane area was 337.5 m^2 and 324.0 m^2, respectively. A mass of 0.067 kg of NaOH per cubic meter of effluent was required for pH adjustment. The monthly volume of HCl 0.2% required for membrane chemical cleaning was 0.39 m^3. The estimated NF power requirement for feed pump was 0.40 kWh/m^3, plus 0.2 kWh/m^3 for the UF unit. Other costs, such as labor and retentate disposal, were not assessed in this work, and neither was the profit for water reuse and environmental valorization.

TABLE 2.12 – Cost estimation of the UF-NF treatment system for AMD

	Description	**Values**	**Units**
System Characteristics	Annual System Capacity	131,040	m^3/year
	Average Permeate Flux	0.025	m^3/h.m^2
	Required UF Membrane Area	337.50	m^2
	Required NF Membrane Area	324.00	m^2
	Design Plant Life	15	Years
	Membrane Lifespan	5	Years
	Brazil Investment Rate	10	%
	Energy Price	0.04	US$/kWh
CapEx	**UF-NF Systems**	**131,250.00**	**US$**
OpEx	UF-NF Membrane Replacement	0.063	US$/$m^3$
	Capital Cost Amortization	0.132	US$/$m^3$
	Alkalizing Agent (pH = 5.5)	0.028	US$/$m^3$
	Cleaning Agent	0.005	US$/$m^3$
	UF-NF Energy Requirement	0.024	US$/$m^3$
	Maintenance	0.007	US$/$m^3$
	Total	**0.257**	**US$/$m^3$**

The total capital cost (CapEx) of the NF system was estimated at 131,250.00 US dollars and the total operational cost (OpEx) at 0.257 US dollars per cubic meter of effluent. These values are similar to those indicated in the literature. Gorenflo *et al.* (2002) reported that for the nanofiltration (NF200B – Filmtec/Dow) of 7,300,000 m^3/year of pretreated groundwater, with high hardness and NOM content, the CapEx and OpEx were 6,897,000 € and 0.23 €/m^3, respectively. And Costa and De Pinho (2006) obtained for the nanofiltration (NF200B-400 – Filmtec/Dow) of 100,000 m^3/day of surface water for drinking water production a CapEx and OpEx of 17,610,716 € and 0.214 €/m^3, respectively.

Finally, the price of the alkalizing agent represented 11% of the total OpEx. Caustic soda is an expensive alkalizing agent and industries usually apply soda ash, lime, or limestone to increase effluent pH. However, because of the increased acidity of the effluent (the effluent from the first collection had and acidity of 188.10 mg $CaCO_3$/L), the high cost for pH adjustment was expected. Moreover, the effluent pH would have to be increased for either water reuse or effluent discharge; therefore, this cost was independent of the AMD treatment method selected.

2.4 Conclusions

- MF/UF was selected as the most appropriate pretreatment for NF/RO treatment, since it improved the quality of the final permeate and reduced the fouling tendency.
- In comparison, NF was more suitable for AMD treatment than RO because of the extremely low permeate fluxes of the RO membranes (10.0 and 10.2 L/h.m^2 for the BW30 and TFC-HR membranes, respectively), which increased the initial investment cost of the membrane system. Among the NF membranes, the NF90 had the highest retention efficiency (99.7% for sulfate and 99.0% for calcium), and the NF270 had the highest permeate flux (88.6 L/h.m^2).
- The NF270 membrane at pH 5.5 was selected as the most promising for AMD treatment because it had the lowest fouling tendency (fouling resistance at 40% water recovery rate was $4.15\times10^{+12}$ m^{-1}), the highest permeate flux by water flux (85.3%), and high ionic retention (93.1, 94.9, and 86.1% for calcium, magnesium, and sulfate retentions, respectively).
- The maximum water recovery rate (RR) for a single element at the optimized conditions was 60%. The permeate quality obtained up to a recovery rate of 60% was superior to the

process water quality used by this mining company (i.e., 13.3 mg/L calcium and 262.1 mg/L sulfate). Furthermore, the permeate flux decreased, following the same trend as the effective pressure decrease up to 60% RR. After 60% RR, the permeate flux decrease was sharper, indicating higher membrane fouling.

- The total capital cost (CapEx) of the NF treatment system was estimated at US$ 131,250.00, and the total operational cost (OpEx) was 0.257 US$/$m^3$ of effluent.

3 CHAPTER

ACID MINE DRAINAGE TREATMENT BY NANOFILTRATION: A STUDY OF MEMBRANE FOULING, CHEMICAL CLEANING, AND MEMBRANE AGEING

3.1 Introduction

Acid mine drainage (AMD) is an effluent formed during the oxidation of sulfide minerals found in mining waste, tailings, and mine structures of abandoned or active mines (Anawar, 2013). AMD is characterized by low pH, high sulfate concentration (SO_4^{-2}), and variable concentrations of metals and metalloids. Nanofiltration (NF) and reverse osmosis (RO) are established technologies for heavy metal retention, and recent studies have successfully applied membrane separation processes (MSP) to treat synthetic and real AMD (Mullett *et al.*, 2014). Moreover, NF has been suggested as the preferable membrane separation process for effluent treatment due to its higher permeate flux, lower required pressure and energy consumption, and lower capital investment and operational cost (Fornarelli *et al.*, 2013). In terms of composition, the RO and NF membranes most widely used nowadays are polyamide (PA)-based thin-film composite (TFC) membranes. These membranes provide high selectivity and water permeability; however, they may be degraded by a number of chemicals, including chlorine (Do *et al.*, 2012). In Chapter 2, the treatment of gold AMD by MSP was evaluated. The pretreatment, type of process, commercial membrane, feed pH, and water recovery rate were assessed. The best operational conditions were found with the NF membrane, NF270, treating pretreated AMD (microfiltration or better) at pH 5.5 and with a maximum water recovery rate of 60%. The permeate obtained at these operational conditions was suitable for industrial reuse.

In MSP, the rejection of solution components inevitably places a constraint on all pressure-driven processes. The rejected components tend to accumulate at the membrane surface leading to a decrease in permeate flux or an increase in transmembrane pressure (defined as the difference between the applied pressure (ΔP) minus the osmotic pressure difference between the retentate and permeate sides of the membrane ($\Delta\pi$)) (Judd, 2010). This accumulation of solution components is known as membrane fouling and is caused by the deposition of organic and inorganic matter and/or the formation of biofilms on the membrane surface (Simon, Mcdonald, *et al.*, 2013). Despite the numerous studies on the subject, membrane fouling is inevitable and a major problem in NF application (Wei *et al.*, 2010). Because membrane fouling causes a decline in productivity, deteriorates permeate quality, increases energy consumption and treatment cost, and shortens membrane lifespan, it must be controlled for an economically feasible operation (Ang *et al.*, 2011).

Membrane fouling can be removed partially by physical or chemical cleaning. Membrane physical cleaning methods include hydraulic cleaning (back pulse and back flush), ultrasonic vibration, air or CO_2 sparging, and back permeation (Regula *et al.*, 2014). Physical cleaning methods are less expensive than chemical cleaning methods. They also provide many other advantages over chemical cleaning, such as high cleaning process velocity (usually less than 2-min duration), low chemical demand, and no chemical waste to be disposed of; moreover, physical cleaning is less likely to degrade the membrane and/or decrease the membrane lifespan (Judd, 2010). Physical cleaning is performed at regular intervals and removes most of the reversible membrane fouling. However, its efficiency tends to decrease during membrane operation, as more irreversible membrane fouling accumulates at the membrane surface. Once this occurs, chemical cleaning is recommended (Vanysacker *et al.*, 2014).

Membrane chemical cleaning involves both chemical and physical interactions. Chemical interactions are related to the reaction between the cleaning agent and the fouling layer. This reaction lessens the structural integrity of the fouling layer, thus facilitating its mechanical removal. In contrast, physical interactions are related to the mass transport of components from the bulk solution to the membrane surface and from the membrane surface to the bulk solution (Sohrabi *et al.*, 2011). Periodic chemical cleaning often represents the only way to partially restore the initial permeate flux (Klüpfel and Frimmel, 2010). There is a large variety of membrane cleaning chemicals commercially available that are typically divided into alkaline cleaners (e.g., sodium hydroxide (NaOH)); acid cleaners (e.g., hydrochloric acid (HCl), phosphoric acid (H_3PO_4), and citric acid); surfactants (e.g., tetra-sodium ethylene diamine tetraacetic acid (Na_4EDTA), and sodium dodecyl sulfate (Na-SDS)); and salt solutions (e.g., NH_2SO_3H and $Na_2S_2O_4$). Alkaline cleaners are usually recommended for organic-fouled membranes and acid cleaners for membranes fouled with inorganic salts. Surfactants have hydrophilic and hydrophobic groups and are, therefore, soluble in both organic and aqueous solvents. They solubilize and remove macromolecules in the fouling layer by forming micelles around them. Inert salt solutions can be used as an alternative for cleaning membranes fouled by gel-forming hydrophilic organic foulants (Ang *et al.*, 2011). Thus, the selection of the best cleaning agent is related directly to the foulants identified, or expected, on the membrane surface. The membrane material also must be considered when selecting a cleaning agent because some combinations of cleaning agent and membrane material may result in the irreversible loss of membrane performance and shorten the membrane lifespan. Other factors that need to be considered during membrane chemical

cleaning are cleaning agent concentration and pH; system temperature, pressure, and flow rate; and cleaning time (Wei *et al.*, 2010; Simon, Price, *et al.*, 2013).

Although essential in any NF/RO application, chemical cleaning may accelerate the membrane ageing process (Simon, Price, *et al.*, 2013). Membrane ageing is considered as the changes from the initial state and properties of the membrane over time. It is a comparative analysis, which cannot be determined quantitatively. Membrane ageing depends on the operational conditions of both the process and the cleaning step. Moreover, membrane aging can result in a decrease in process productivity, an increase in required physical and chemical cleaning frequency, modification of the membrane physicochemical properties (such as membrane hydrophobicity and surface roughness), alteration of membrane selectivity, and loss of integrity (Regula *et al.*, 2014).

Membrane chemical cleaning has been fairly studied. Wei *et al.* (2010) studied the Desal-5 DK membrane (Osmonics, USA) fouling process during complex pharmaceutical wastewater treatment and then evaluated the chemical cleaning process based on the identification of the membrane foulants. The complex pharmaceutical wastewater was characterized by high chemical oxygen demand (COD), total dissolved solids (TDS), and inorganic ions (such as Na^+, Ca^{2+}, SO_4^{2-}, and HCO_3^-). After 3 h of operation, some calcium sulfate and calcium carbonate foulants appeared on the membrane surface; moreover, these salts content increased after 180 h of operation. Membrane chemical cleaning tests showed the following order for cleaning efficiencies: NaOH (pH 11) < HCl (pH 2) < citric acid (pH 2) < Na_4EDTA (10 mM). Ang *et al.* (2011) investigated the effect of different RO cleaning modes after membrane fouling of the LFC-1 membrane (Hydranautics, Oceanside, CA) during wastewater treatment. The cleaning solutions studied were NaOH, disodium ethylene diamine tetraacetate (Na_2EDTA), sodium dodecyl sulfate (SDS), and sodium chloride (NaCl). The sequence or combination of two cleaning agents was compared to the use of one cleaning agent. It was observed that the addition of NaOH enhanced the overall cleaning performance when introduced with other chemical agents, due to its ability to loosen the organic fouling layer. However, as far as we know, no study has been published specifically on the cleaning process of membranes fouled during AMD treatment.

Simon *et al.* (2012) studied the effect of chemical cleaning with four cleaning solutions (NaOH, citric acid, SDS, and EDTA) at three different solution concentrations on virgin

NF270 membranes (Dow Filmtec™, Minneapolis, MN, USA). They measured the membrane zeta potential, hydrophobicity, permeability, and solutes rejection before and after membrane exposure to the cleaning solution for 18 h at 35 °C. Many differences were observed in the membrane characteristics due to membrane ageing by the cleaning solution. The salt rejection decreased especially with caustic cleaning at all concentrations and with acidic cleaning at pH 1.5. In a later study, Simon, Price, *et al.* (2013) evaluated the effect of cleaning temperature on NF270 membrane ageing. The same cleaning solutions were tested for 18 h and the cleaning temperature was set at 20, 35, or 50 °C. They concluded that the cleaning temperature did not exert any discernible impact on the surface charge of the NF270 membrane, but amplified or reduced the impact on other membrane properties (such as hydrophobicity, surface roughness, and water permeability) as well as solute rejection. Do *et al.* (2012) assessed the degradation of PA membranes (NF90, BW30, and NF270; Dow Filmtec™) by prolonged hypochlorite exposure at different solution concentrations and exposure time. Membrane characterization and performance tests were conducted. X-ray photoelectron spectroscopy (XPS) results showed that chlorine attachment onto the PA surface decreased in the following order: NF90 > BW30 > NF270. However, no study of membrane ageing by HCl or other acid solutions was found in the literature.

Therefore, the aim of this study was to investigate NF membrane fouling during AMD treatment and the cleaning efficiency of different chemical cleaning agents to this fouling layer. AMD has low concentrations of organic components, and thus, it was expected to form a fouling layer different from those assessed in other studies. Moreover, this study aimed to evaluate the membrane ageing caused by prolonged contact with the AMD effluent, the best cleaning agent solution, and the best combination of both solutions.

3.2 Materials and Methods

3.2.1 Effluent Characterization

AMD was collected on the fourth level below ground of an underground gold mine in the state of Minas Gerais, Brazil. AMD characteristics vary throughout the year, and the main properties of the two samples used for this study are presented in TABLE 3.1.

TABLE 3.1 – AMD main characteristics

AMD	pH	Conductivity (µS/cm)	Total Solids (mg/L)	Sulfate (mg/L)	Chloride (mg/L)	Calcium (mg/L)	Magnesium (mg/L)
1st collection	3.76	2,573	3,102	1,959.5	151.5	284	226
2nd collection	3.35	2,965	3,432	2,767.7	14.1	309	114

3.2.2 Unit Description

Ultrafiltration (UF) was conducted on a commercial submerged membrane module (ZeeWeed) with a filtration area of 0.047 m^2, polyvinylidenefluoride (PVDF)-based polymer composition, and average pore diameter of 0.04 µm. UF occurred at 0.7 bar and up to 60% of water recovery rate.

NF tests were carried out in a bench-scale unit. This unit comprised one supply tank (ST), one pump, one valve for pressure adjustment, one rotameter, one manometer, one thermometer, and one stainless steel membrane cell. The stainless steel membrane cell had a 9.8 cm diameter, providing a filtration area of 75 cm^2, a more complete description of this unit can be found on Section 2.2.3.2. The flat sheet PA thin-film composite membrane NF270 from DOW Filmtec™ was used in this study. This membrane is a loose NF membrane with relatively low salt rejection. Initially this membrane was inserted onto the membrane cell and pre-compacted with distilled water at 10 bar, until permeate flux stabilization. All effluent filtration tests were conducted at 10 bar, feed flow rate of 0.14 m^3/h, and approximate temperature of 25 °C.

3.2.3 Membrane Characterization

Prior to characterization, the virgin NF270 membrane (referred to as "V-NF270" from now on, with V for "virgin") was immersed in a citric acid solution at pH 2.5 and then in a NaOH solution at 0.1%, both in an ultrasonic bath for 20 min each. Then, all membranes (from the experiments and virgin) were cleaned with deionized (DI) water and dried at ambient temperature (approximately 25 °C). The morphological and chemical characterizations of the NF membranes of interest were carried out by the following analysis: scanning electron microscopy (SEM) with energy dispersive X-ray (EDX) spectroscopy, atomic force microscopy (AFM), water contact angle, and attenuated total reflectance Fourier transform infrared (ATR/FTIR) spectroscopy.

3.2.3.1 SEM/EDX Spectroscopy

Images of the membrane surface were obtained by SEM and the content of the surface elements was analyzed by EDX spectroscopy. Prior to these analyses, the membranes were coated with a 5-nm carbon layer by a sputter coating machine (Leica EM SCD 500 with a pressure of 10^{-2}–10^{-3} mbar and current of 2.5 A). SEM/EDX experiments were conducted with an FEI Quanta 200 scanning electron microscope for membrane ageing and with a JEOL JSM-6360LV scanning electron microscope for scaling evaluation.

3.2.3.2 AFM Spectroscopy

AFM can be used to determine the roughness of the membrane surface. AFM experiments were conducted with an MFP-3D-SA microscope (Asylum Research) equipped with an AC160TS probe. The scan rate was 1.00 Hz, 256 points and lines were taken, and a 5×5 μm area was analyzed. At least three images were obtained for each membrane.

3.2.3.3 Water Contact Angle Measurement

Water contact angle measurement was used to evaluate possible changes in the membrane hydrophobicity. The water contact angle was determined with a Digidrop-DI goniometer (GBX Instruments) equipped with a CCD camera and an automated liquid dispenser, using the standard sessile drop method. At room temperature, 6 μL of DI water droplets were placed on the membrane surface, and then the contact angle was measured. For average determination, five droplets were applied to each membrane.

3.2.3.4 ATR/FTIR Spectroscopy

ATR/FTIR spectroscopy was conducted to evaluate changes in the chemical bonds of the membrane surface. ATR/FTIR spectroscopy was carried out in Shimadzu FTIR (model IR Prestige-21) with a Dura SamplIR II™ detector (Smiths). The spectrum was obtained in the range of 400–4000 cm^{-1} at 2 cm^{-1} resolution. The results were converted from transmittance mode (T) to absorbance mode (A) by means of EQUATION 20.

$$A = -\log(T) \qquad \text{(Eq. 20)}$$

3.2.4 Scaling Evaluation during AMD Treatment

The main foulants of the NF270 membrane during AMD treatment were analyzed after 7 h of operation. AMD from the second collection was used. Initially, two virgin membranes, after

the cleaning procedure with citric acid and NaOH, were placed in a duplicate NF unit; this unit had two identical membrane cells. The AMD had its pH adjusted to 5.5 with NaOH 5.0 N and was pretreated with UF. Then, 2 L of this pretreated AMD were placed in the unit supply tank and NF was carried out simultaneously in both membrane cell units as described in Section 3.2.2. The permeate was collected for analysis, whereas the retentate was continuously returned to the supply tank. Every time the volume on the supply tank dropped below 800 mL, 500 mL of pretreated AMD was added to the supply tank; this procedure was repeated 15 times, providing 7 h of continuous operation. The membrane from the first membrane cell was cleaned with distilled water, and will be referred to as "F-NF270" from now on, with F for "fouled". The cleaning procedure with distilled water consisted of 30 min of water recirculation at 0 bar, feed flow rate of 0.14 m^3/h, and approximate temperature of 25 °C, this cleaning procedure will be referred to as hydrodynamic cleaning. The membrane from the second membrane cell was first hydrodynamically cleaned, then it was cleaned with an acidic cleaning solution (0.5% w/w HCl) for 1 h at 1.5 bar, feed flow rate of 0.14 m^3/h, and approximate temperature of 25 °C, and then it was hydrodynamically cleaned again. This membrane will be referred to as "FAC-NF270" from now on, with FAC for "fouled after cleaning". These membranes were characterized by SEM/EDX, AFM, water contact angle, and ATR/FTIR analysis.

Half of the F-NF270 membrane and a piece of the V-NF270 membrane were immersed in an ultrasonic bath for 24 h in an aqua regia solution (HCl and HNO_3 at 3:1 v/v) for acid digestion. The aim was to dissolve, remove, and characterize most of the inorganic foulants from the membrane surface. The concentrations of inorganic cations were analyzed with an ICP optical emission spectrometer (Varian 720-ES with a CCD detector axial view).

3.2.5 Chemical Cleaning Optimization

Initially, the NF270 membranes were cleaned with citric acid solution at pH 2.5 and then NaOH solution at 0.1%. Then, these membranes were inserted on the membrane cell and pre-compacted with distilled water at 10 bar. As small variations in temperature can alter water permeability, flux normalization to 25 °C (J_N) was accomplished by means of a correction factor associated with water viscosity. The initial membrane water permeability ($K_{Initial}$) was obtained from the slope of normalized permeate flux of pure water (J_N) versus applied pressure (ΔP) at 10.0, 8.0, 6.0, and 4.0 bar as shown in EQUATION 21.

$$K_{Initial} = \frac{J_N \cdot \mu(T)}{\Delta P \cdot \mu(25^{\circ}C)} \quad \text{(Eq. 21)}$$

where $\mu(T)$ is water viscosity at the process temperature, and $\mu(25\,^{\circ}C)$ is water viscosity at 25 °C.

AMD treatment was then carried out. Initially, the effluent pH was adjusted to 5.5 with NaOH 5.0 N and pretreated with UF. Then, NF was carried out with the NF270 membrane for 4 h at 10 bar, feed flow rate of 0.14 m^3/h, and approximate temperature of 25 °C. The permeate was collected and the retentate returned to the feed tank. The fouled membrane water permeability (K_{Fouled}) was obtained after AMD NF from the slope of the normalized permeate flux of pure water versus applied pressure at 10.0, 8.0, 6.0, and 4.0 bar. Finally, the fouled membrane was cleaned, and the membrane water permeability after the cleaning procedure ($K_{After\ Cleaning}$) was obtained from the slope of normalized permeate flux of distilled water by applied pressure at 10.0, 8.0, 6.0, and 4.0 bar.

The membrane cleaning efficiency (η) was calculated from the obtained water permeabilities, as shown in EQUATION 22 (Sohrabi *et al.*, 2011):

$$\eta(\%) = \frac{K_{After\ Cleaning} - K_{Fouled}}{K_{Initial} - K_{Fouled}} \cdot 100\% \quad \text{(Eq. 22)}$$

3.2.5.1 Cleaning Agent Investigation

The cleaning efficiency of seven chemical cleaning agents to remove the AMD fouling layer was assessed. AMD from the first collection was used. The cleaning agents tested were anhydrous citric acid (2% w/w, pH=2.1), hydrochloric acid (HCl) (0.2% w/w, pH=1.3), phosphoric acid (H_3PO_4) (0.5% w/w, pH=1.8), sulfuric acid (H_2SO_4) (0.1% w/w, pH=1.8), nitric acid (HNO_3) (0.2% w/w, pH=1.5), sodium hydroxide (NaOH) (0.4% w/w, pH=13.0), and disodium ethylene diamine tetraacetate (Na_2-EDTA) (1% w/w). The cleaning procedure consisted of static cleaning for 1 h followed by cleaning solution recirculation for 30 min at a pressure of 1.5 bar, feed flow rate of 0.14 m^3/h, and approximate temperature of 25 °C.

An estimation of the chemical cleaning cost per procedure was conducted. Considering the effluent volumetric flow of 15 m^3/h, a recovery rate equal to 90% for UF (effluent pretreatment) and 60% for NF, and the average permeate flux of 25 L/h.m² for NF; the required membrane area for NF was 324.0 m^2, or 9 modules of NF with active surface are

equal to 37 m^2. The volume of cleaning solution required for a cleaning procedure was equal to the membrane module volume (0.03 m^3) multiplied by the number of modules required for the AMD treatment, plus the estimated volume of the feed and return pipes. Cleaning agent prices were based on an estimate provided by a large chemical supplier[3]. HCl (37%), H_3PO_4 (85%), H_2SO_4 (98%), and HNO_3 (70%) prices were provided per 200 L of solution, whereas anhydrous citric acid, NaOH, and Na_2-EDTA prices were provided per 45 kg of chemical agent.

3.2.5.2 Cleaning Agent Concentration

Cleaning agent concentrations directly influence the cleaning efficiency, thereby affecting the cleaning procedure duration. The cleaning efficiencies of HCl at concentrations of 0.05%, 0.10%, 0.20%, 0.50%, and 1.00% were tested for 15- and 30-min cleaning periods. AMD from the second collection was used. The NF270 membrane exposure to HCl was calculated for each solution concentration.

3.2.6 Membrane Ageing

Membrane ageing was evaluated in terms of separation characteristics and morphological and chemical characteristics of the membrane. The measured separation characteristics were water permeability, magnesium sulfate ($MgSO_4$) rejection, and glucose rejection. Water permeability was obtained from the linearization of the ratio of temperature-normalized permeate flux of pure water (J_N) by applied pressure (ΔP) at 10.0, 8.0, 6.0, and 4.0 bar. $MgSO_4$ rejection was measured at 15% recovery rate, 5 bar applied pressure, and room temperature (25 °C). A $MgSO_4$ solution of 2,000 ppm was fed to the NF system. The observed $MgSO_4$ rejection was obtained indirectly from conductivity measurements of the feed solution and accumulated permeate (Hanna conductivity meter HI 9835). Lastly, glucose rejection was measured at 10% recovery rate, 10 bar applied pressure, and 25 °C. The glucose feed solution had an approximate concentration of 500 mg/L. The observed glucose rejection was obtained indirectly from carbohydrate concentration of the feed solution and accumulated permeate. Carbohydrate analysis was conducted by the colorimetric method of Dubois et al. (Dubois *et al.*, 1956). Analyses of morphological and chemical characteristics involved consisted of SEM/EDX, AFM, water contact angle, and ATR/FTIR. Each of these tests was

[3] Value available at: < https://www.spectrumchemical.com>. Accessed on: 13 October 2015.

carried out with a piece of the V-NF270 membrane and with the NF270 membrane at the end of each experiment.

The first test evaluated NF270 membrane ageing by long-term exposure to AMD retentate. A virgin NF270 membrane was immersed in the AMD retentate obtained at 60% water recovery rate (i.e., the feed solution was concentrated approximately 2.5 times). The AMD retentate solution was changed every 30 days to maintain solution characteristics. Before immersion in the new retentate solution, the membrane was placed in the bench-scale NF unit, and water permeability, $MgSO_4$ rejection, and glucose rejection were measured. This process was continued for 270 days. Membrane samples were collected for surface evaluation by SEM/EDX (90 d), AFM (270 d), water contact angle (270 d), and ATR/FTIR (240 d).

The second test aimed to evaluate the membrane ageing that would happen during real AMD treatment. Thus, the long-term exposure to the AMD retentate was combined with periodic exposure to a HCl solution to simulate the periodic chemical cleaning procedure. The virgin NF270 membrane was immersed in the AMD retentate (60%). Every 30 days, before changing the AMD retentate solution, the membrane was immersed for 1 day in 1.0% HCl solution. Then, water permeability, $MgSO_4$ rejection, and glucose rejection were measured before the membrane was placed in a new AMD retentate solution. This process was continued for 270 days. Membranes samples were collected for surface evaluation by SEM/EDX (90 d), AFM (270 d), water contact angle (270 d), and ATR/FTIR (240 d).

3.3 Results and Discussion

3.3.1 Scaling Evaluation during AMD Treatment

The NF270 membrane fouling layer was evaluated during 7 h of operation with ultrafiltrated AMD at pH 5.5. This condition was previously determined as the most promising for gold AMD treatment (Chapter 2). FIGURE 3.1 shows the permeate flux decay with filtration time for each filtration cell. The flux decay is a result of membrane fouling and the increase of the retentate osmotic pressure. After 7 h of treatment, the permeate flux had decreased 65% for the first membrane cell and 60% for the second membrane cell.

FIGURE 3.1 – Permeate flux decay during AMD treatment

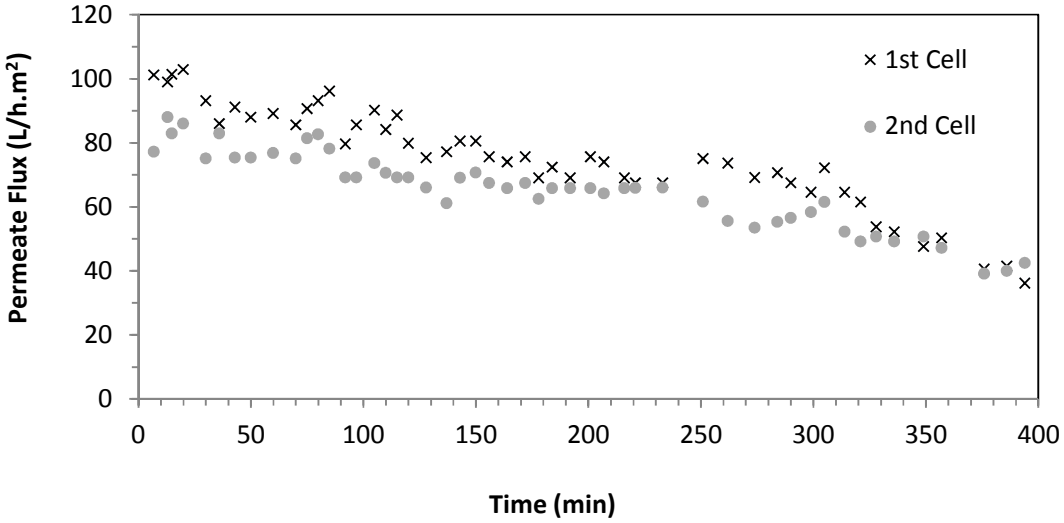

TABLE 3.2 shows the main inorganic cations concentrations of the solution of V-NF270 membrane and F-NF270 membrane after acid digestion with aqua regia. As can be seen from TABLE 3.2, the F-NF270 membrane had a higher concentration of every cation per mass of membrane than the V-NF270 membrane. The adsorbed ions and the fouling layer of the F-NF270 membrane were removed during acid digestion. Some observed cations were expected to be adsorbed ions, such as arsenic, lead, chromium, and nickel, since these cations had very low concentration in the raw AMD but relatively high concentration in the F-NF270 solution. On the other hand, cations such as aluminum, calcium, iron, magnesium, and manganese can form precipitates and oxides and, therefore, were expected to be the main foulants at the membrane surface.

TABLE 3.2 – Cations concentrations of the solutions of the acid digestion of the V-NF270 and F-NF270, and of the raw AMD

Cations (mg/g of membrane)	AMD (mg/L)	V-NF270	F-NF270
Aluminum	13.646	0.063	0.344
Arsenic	0.181	0.026	0.598
Calcium	366.62	0.57	1.19
Lead	0.1862	0.0030	0.0507
Cobalt	0.2441	0.0056	0.0098
Copper	0.1618	0.0327	0.0823
Chromium	< 0.010	0.009	0.428
Iron	2.98	0.57	3.39
Magnesium	298.650	0.025	0.136
Manganese	18.636	0.015	0.040
Nickel	0.7673	0.0029	0.2088
Potassium	10.65	0.14	2.99
Sodium	10.65	1.10	1.01
Zinc	3.581	0.029	0.106

FIGURE 3.2 shows the SEM images of the F-NF270 [FIGURE 3.2(a)] and FAC-NF270 [FIGURE 3.2(b)] membranes at two magnifications. The V-NF270 membrane usually has a flat and homogeneous surface, without the presence of visible corrugations at the membrane surface. The image of the F-NF270 membrane, however, shows many irregularities. These irregularities are a result of the fouling layer of precipitates formed during the AMD treatment. EDX analyses of the precipitates found at two different points are shown in FIGURE 3.3. These images confirmed the presence of many cation foulants that were observed during the ICP analyses. However, the EDX selects a specific area or point for analysis, whereas the ICP gives a broader picture of the cations present at the membrane surface. The FAC-NF270 membrane, on the other hand, was more regular with just a few small irregularities.

FIGURE 3.2 – SEM images of the membranes: a) F-NF270; b) FAC-NF270, at x10,000 and x5,000 magnifications

a)

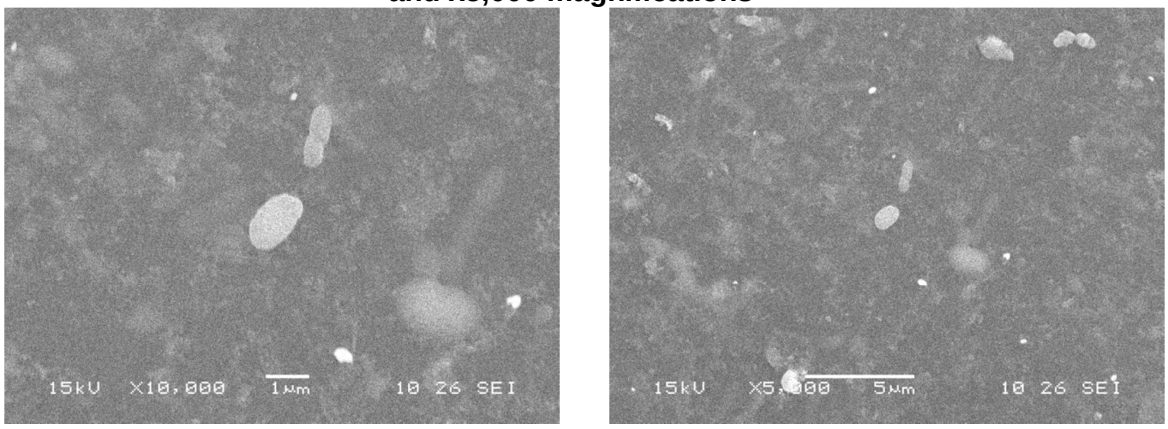

b)

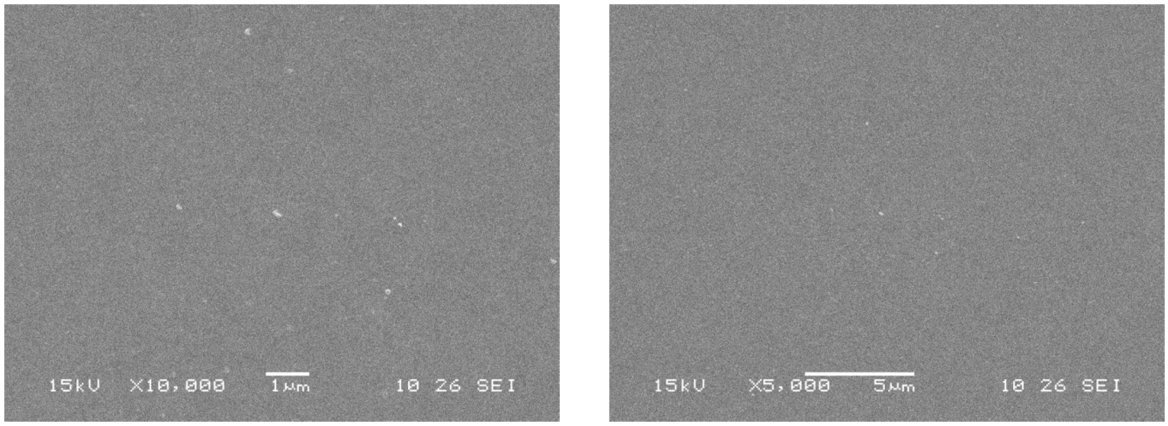

FIGURE 3.3 – EDX of the precipitates found at two different points of the F-NF270

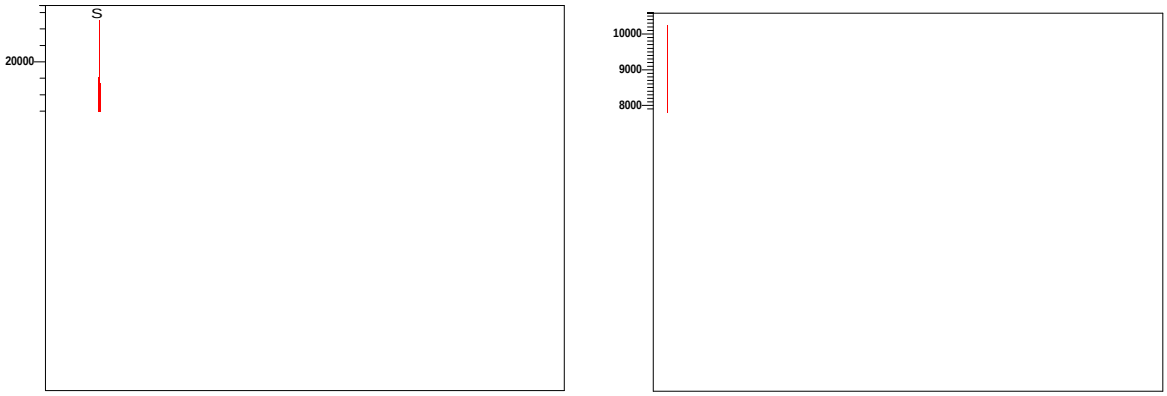

The membrane surface roughness of the V-NF270, F-NF270 and FAC-NF270 membranes was obtained for a 5×5 μm area. TABLE 3.3 shows the root mean square (RMS) roughness results. The measured surface roughness of the V-NF270 membrane was 5.18 ± 0.71. Hilal *et al.* (2005) also measured the NF270 surface roughness in a 2×2 μm area and reported a value of 4.3797 nm. The influence of the AFM probe (or tip) and scan area on surface roughness measurements were evaluated by Sedin and Rowlen (2001). They observed that surface

roughness increased as scan area increased. Moreover, the increase trend depended on the type of probe used, thus explaining the higher surface roughness observed in this experiment.

TABLE 3.3 – NF270 membrane surface roughness and water contact angle

Membrane	RMS Roughness (nm)	Water Contact Angle (°)
V-NF270	5.18±0.71	28.1±1.8
F-NF270	5.22±0.78	61.4±1.2
FAC-NF270	4.62±0.49	36.7±1.9

The NF270 RMS roughness increased after fouling with AMD, and decreased after cleaning with a 0.5% w/w HCl solution. FIGURE 3.4 shows the AFM 3D images of the membranes V-NF270, F-NF270, and FAC-NF270. When these images are compared qualitatively, it can be seen that the V-NF270 membrane peaks are more evenly distributed than the F-NF270 and the FAC-NF270 membrane peaks. The F-NF270 membrane surface is relatively less rough than the V-NF270 membrane; however, the former has frequent periodic high peaks that increased the RMS roughness. These high peaks could be the crystals of foulants (such as $CaSO_4$), which preferentially grew on the membrane surface and on other crystals. Finally, the FAC-NF270 membrane seemed to have a relatively rougher surface than the F-NF270 membrane, but a lower concentration of higher peaks, which decreased the RMS roughness. However, when comparing the concentration and height of the V-NF270 membrane peaks with those from the FAC-NF270 membrane, it is evident that the FAC-NF270 membrane had not returned to its original condition. Thus, the cleaning procedure removed the fouling layer to some extent, especially the high peaks' foulants, but it did not recover the membrane completely. The remaining fouling layer observed on the FAC-NF270 membrane is expected to be mostly irreversible fouling, because even with a 1-h cleaning procedure it was not removed. This result shows the importance of the optimization of the cleaning procedure, both in relation to the cleaning agent and to the solution concentration, for minimizing the residual fouling layer and the cleaning procedure time.

FIGURE 3.4 – AFM images of: a) V-NF270, b) F-NF270, and c) FAC-NF270 membranes

a)

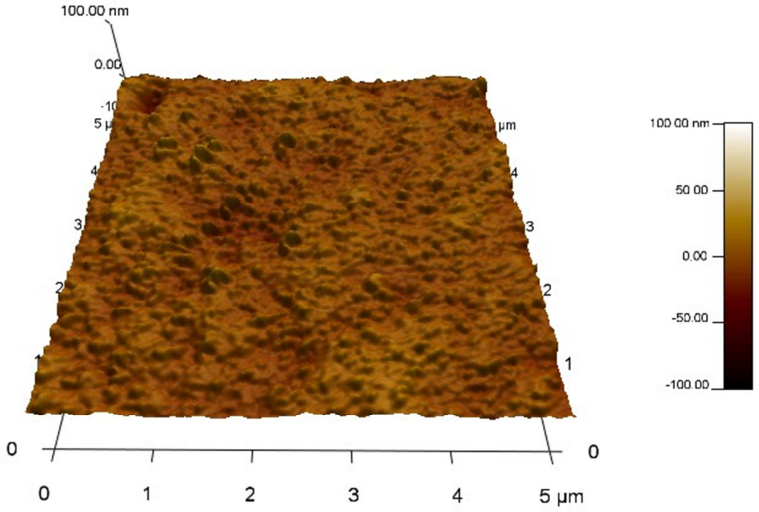

b)

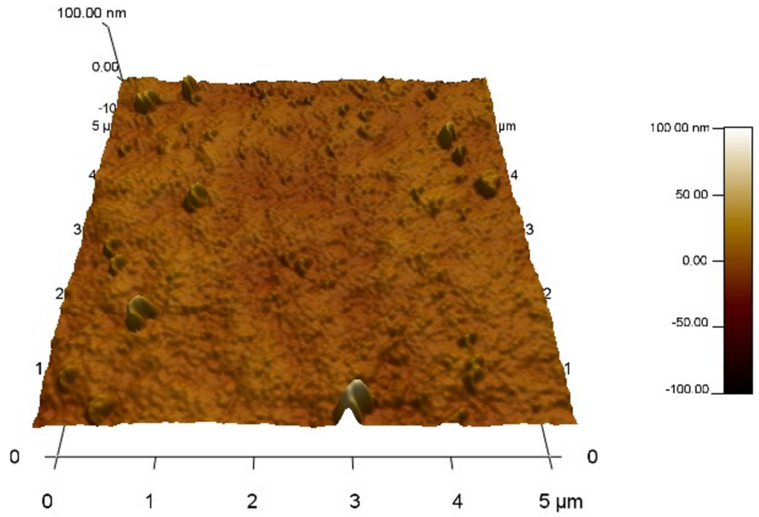

c)

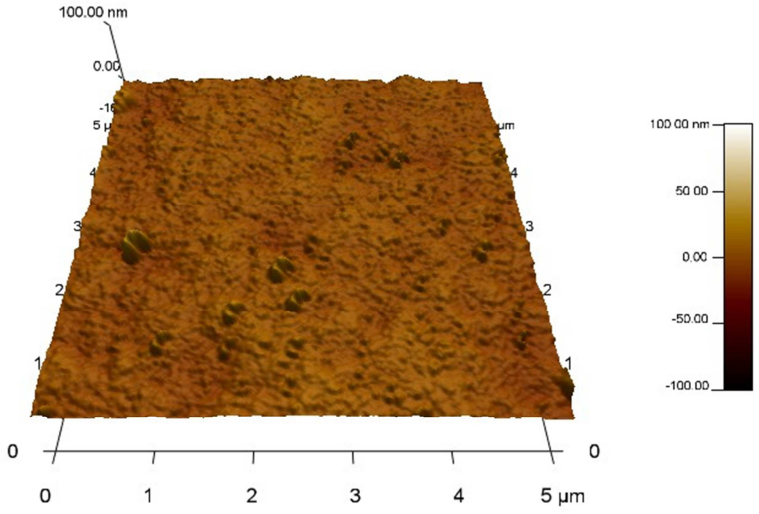

TABLE 3.3 also presents the measured water contact angle of the V-NF270, F-NF270, and FAC-NF270 membranes. The measured water contact angle obtained for the V-NF270 membrane was 28.1±1.8°, similar to that reported by Tu *et al.* (2011) of 28.8±2.4°. The higher

water contact angle of the F-NF270 membrane indicates that it became more hydrophobic after AMD treatment. The membrane hydrophobicity decreased after the cleaning procedure with HCl, as can be seen by the lower water contact angle of the FAC-NF270 membrane. However, it remained higher than the water contact angle of the V-NF270 membrane. These observations are consistent with the water permeability of these membranes, as more hydrophilic membranes favor the sorption of water and raise the water flux (Baker, 2012).

Lastly, the ATR/FTIR results for the V-NF270, F-NF270, and FAC-NF270 membranes are shown in FIGURE 3.5. Wavelength ranged from 400 to 2000 cm−1, as no peaks were obtained outside of this range. Because the penetration depth of the ATR/FTIR spectra at wavelengths lower than 2000 cm–1 is higher than 300 nm, there will be a superposition of the chemical information of the selective top layer and the support layer (Tang et al., 2009). The Dow Filmtec™ membranes are thin-film composite membranes composed of three different layers: a polyester support web, a microporous polysulfone interlayer, and an ultrathin PA selective layer. TABLE 3.4 shows the peaks assigned to polysulfone. The observed peaks of the V-NF270 membrane confirm the informed composition of the microporous interlayer. However, Tang et al. (2009) suggested that the PA selective layer was composed of semi-aromatic poly(piperazinamide), with specific peaks at 1630 and 1730 cm−1. These two peaks were not found in this study. As the PA layer composition is proprietary information, it will not be further discussed. Finally, from FIGURE 3.5, it can be seen that all three tested membranes had the same main peaks and that no substantial new peak was observed. This suggests that gold AMD treatment does not change considerably the chemical bonds of the NF270 membrane.

FIGURE 3.5 – ATR/FTIR spectra of the V-NF270, F-NF270, and FAC-NF270 membranes

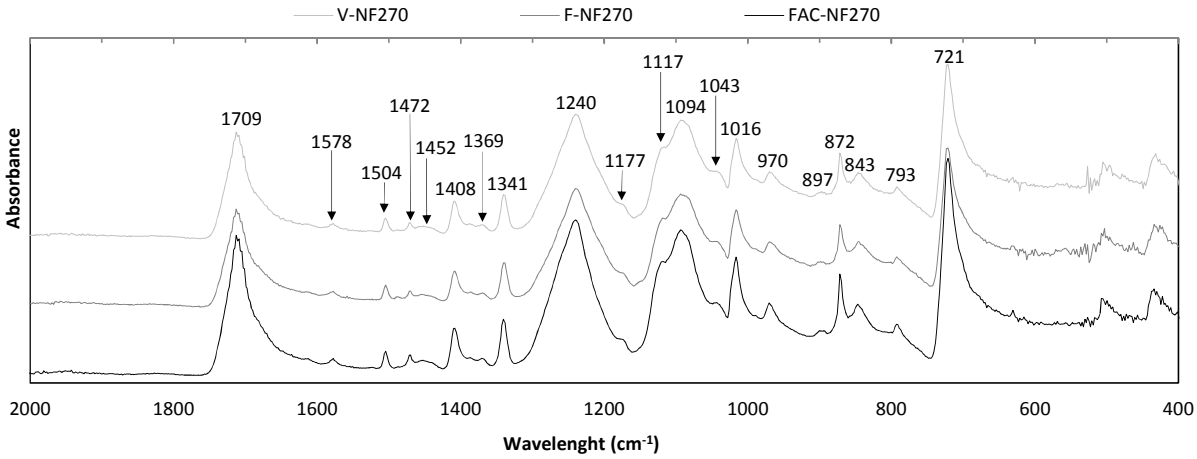

TABLE 3.4 - Peaks assignable from ATR/FTIR spectra to polysulfone

Reported Peaks (cm^{-1})	Observed Peaks (cm^{-1})	Peak Assignments
~1587, 1504, and 1488 [a]	1578, 1504, and 1472	Aromatic in-plane ring bend stretching vibration
1385–1365 [a]	1369	C–H symmetric deformation vibration of $>C(CH_3)_2$
1350–1280 [a]	1341	Asymmetric SO2 stretching vibration
~1245 [a]	1240	C–O–C asymmetric stretching vibration of the aryl–O–aryl group
1180–1145 [a]	1177	Symmetric SO_2 stretching vibration P
~830 [a]	843	In-phase out-of-plane hydrogen deformation of para-substituted phenyl groups

[a] *Apud* Tang *et al.* (2009).

3.3.2 Chemical Cleaning Optimization

3.3.2.1 Cleaning Agent Investigation

FIGURE 3.6 shows the membrane water permeability before membrane fouling ($K_{Initial}$), after membrane fouling (K_{Fouled}), after the first cleaning procedure ($K_{1^{st}Cleaning}$), and after the second cleaning procedure ($K_{2^{nd}Cleaning}$) for a cleaning procedure with citric acid followed by NaOH, and for a cleaning procedure with NaOH followed by citric acid. The membrane water permeability decreased 41% for the citric acid followed by NaOH procedure and 44% for the NaOH followed by citric acid procedure, after 4 hours of AMD treatment due to membrane fouling. The global cleaning efficiency was 68.7% when citric acid was used first and 24.8% when NaOH was used first. The main foulants expected on the membrane surface were inorganic salts. Thus, acid solutions were expected to be more effective cleaning agents than alkaline solutions. The higher overall cleaning efficiency obtained for the cleaning procedure with citric acid first could be explained by the lessening of the structural integrity of the fouling layer upon the reaction of the membrane foulants with the acid solution (Sohrabi *et al.*, 2011). The residual foulants on the membrane surface would then be “loose” and could be removed by the alkaline cleaning. On the other hand, when the alkaline solution was used first, the foulants were strongly attached to the membrane surface and the alkaline solution could not remove it. Therefore, an overall low cleaning efficiency was obtained. The cleaning efficiency of the first cleaning steps were 58.8 and 16.4% for the tests first cleaned with citric acid and NaOH, respectively. These values confirm the low cleaning efficiency of the alkaline solution for AMD foulants. Thus, the use of alkaline solution for AMD foulants as the first cleaning stage or as the second cleaning stage did not show synergy.

FIGURE 3.6 – NF270 membrane water permeability after cleaning procedure with citric acid followed by NaOH and with NaOH followed by citric acid

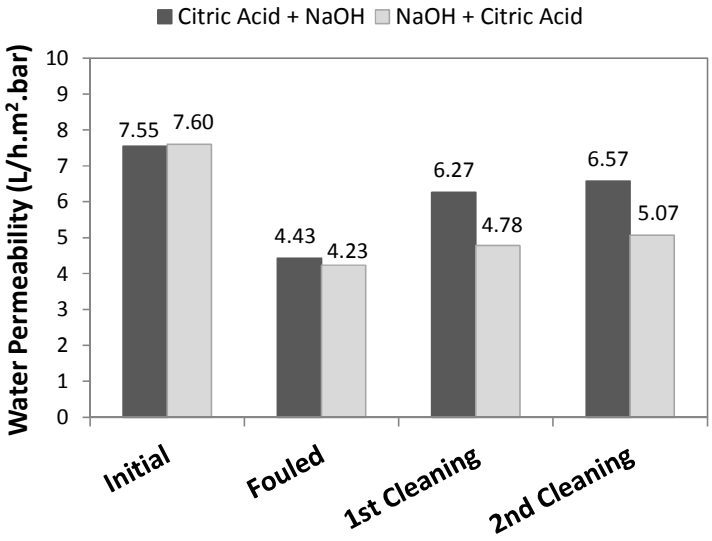

FIGURE 3.7 shows the cleaning efficiency of the evaluated membrane chemical cleaning agents for a single cleaning step. The decrease in the membrane water permeability in these experiments varied from 41% to 48%. This study focused on acidic cleaning solutions because these chemicals are more efficient for AMD-expected foulants. The higher efficiencies of the acidic cleaners (citric, hydrochloric, nitric, phosphoric, and sulfuric acids) in relation to surfactant cleaners (Na_2-EDTA) and alkaline cleaners (NaOH) confirmed this hypothesis. Moreover, Simon *et al.* (2012) reported a decrease in NF270 membrane conductivity rejection after membrane cleaning with an alkaline solution (NaOH) at pH 11. A decrease in conductivity rejection was reported for acidic solutions (citric acid) only at a pH as low as 1.5. Among the evaluated acidic cleaning solutions of this study, the sulfuric and phosphoric acids showed the lowest cleaning efficiencies (respectively 31.2% and 39.6%). The increase of sulfate and phosphate concentrations on the membrane surface may lead to the formation of salts with low solubility in the presence of cations such as Ca^{+2} and Mg^{+2}. The highest cleaning efficiency (73.5%) was obtained with 0.2% HCl.

FIGURE 3.7 – NF270 membrane cleaning efficiency for a single cleaning step.

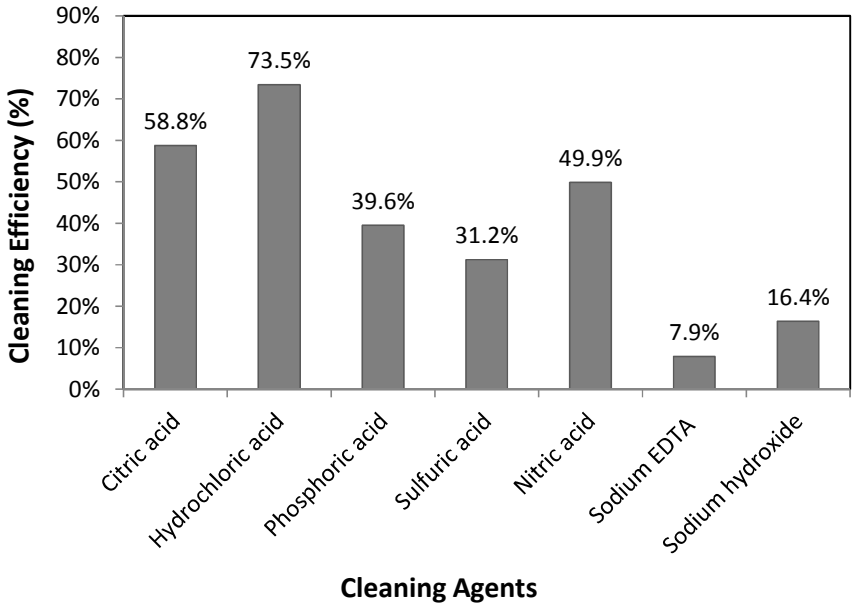

The estimated volume of the membrane modules was 0.27 m^3, and of the pipes was 0.11 m^3. TABLE 3.5 shows the unit price per weight of cleaning agent, the required mass of reagent per cleaning, and the respective price per cleaning. The highest price per cleaning agent mass was obtained for the surfactant EDTA (US$60.32/kg), which also showed the lowest cleaning efficiency (7.9%), followed by the citric acid (US$24.15/kg). The high concentration of citric acid used in this study results in a high price per cleaning for this chemical (US$187.73/cleaning). Furthermore, the cleaning efficiency of citric acid was close to that of H_3PO_4 and lower than HCl. The lowest prices per cleaning agent mass were obtained for H_2SO_4 and HNO_3, respectively US$2.19 and US$5.00 per kg of chemical. Moreover, most of the mining industries produce H_2SO_4 during their activity; therefore, this chemical would have an even lower price. However, the low cleaning efficiency of H_2SO_4 and the possible formation of salts with low solubility with sulfate discourage its use as a membrane-cleaning agent. Among the conditions tested (excluding H_2SO_4), HNO_3 and HCl showed the lowest price per cleaning procedure (US$5.00 and US$12.64, respectively). Because the cleaning efficiency of HCl (0.2%) was 32% higher than that of HNO_3 (0.2%), it was chosen as the best chemical cleaning agent for the NF270 membranes after gold AMD treatment.

TABLE 3.5 – Estimated price of chemicals per chemical cleaning procedure

Cleaning Agent	Price per Weight of Cleaning Agent (US$/kg)	Weight of Cleaning Agent per Cleaning (kg)	Price per Cleaning (US$)
Citric Acid (2.0%)	24.15	7.77	187.73
Hydrochloric Acid (HCl) (0.2%)	16.26	0.78	12.64
Phosphoric Acid (H_3PO_4) (0.5%)	14.87	1.94	28.89
Sulfuric Acid (H_2SO_4) (0.1%)	5.62	0.39	2.19
Nitric Acid (HNO_3) (0.2%)	6.43	0.78	5.00
Na2-EDTA (1.0%)	60.32	3.89	234.43
Sodium Hydroxide (NaOH) (0.4%)	14.75	1.55	16.88

* Chemical prices based on information shared by one chemical supplier; prices may vary from region to region.

3.3.2.2 Cleaning Agent Concentration

FIGURE 3.8 shows the cleaning efficiencies of the NF270 membrane fouled during AMD NF after chemical cleaning was carried out with 0.05%, 0.10%, 0.20%, 0.50%, and 1.00% of HCl for 15 and 30 min. Higher cleaning-agent concentrations led to higher cleaning efficiency for both cleaning intervals. After 30 min of a cleaning procedure, the cleaning efficiency with 1.00% w/w HCl solution was 77.4%. Sohrabi *et al.* (2011) also observed an increase in the cleaning efficiency at higher concentrations of cleaning agents. However, they warned that for some cleaning agents increasing the concentration above a critical value might not increase the cleaning efficiency but rather decrease it. This decrease was not observed with HCl cleaning solution up to a concentration of 1.00%.

FIGURE 3.8 – NF270 membrane cleaning efficiency for different HCl concentrations at 15 and 30 min of chemical cleaning.

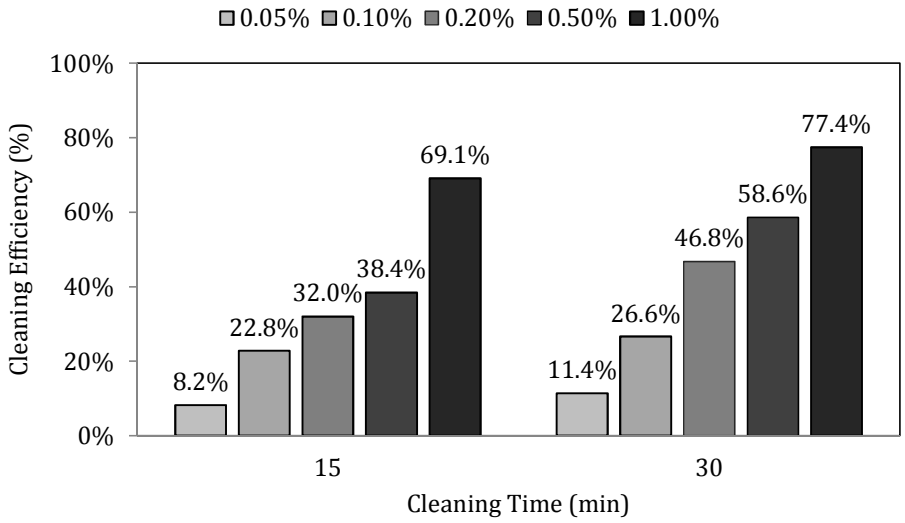

Membrane ageing induced by cleaning procedure is often assessed by the accelerated ageing method, which measures the cleaning agent concentration per time of membrane-cleaning agent contact. This method considers that ageing caused by high solution concentration for a short time is equal to the ageing caused by low solution concentration for a long time period. However, although very used, a good correlation between the laboratory accelerated ageing and the observed natural ageing is not always observed (Regula *et al.*, 2014).

In this study, the cleaning procedure time required to attain a cleaning efficiency of 90% for each solution concentration was estimated based on the cleaning efficiencies at 15 and 30 min for each concentration. The results were used to calculate the membrane exposure to the HCl required until 90% cleaning efficiency per cleaning procedure was achieved (TABLE 3.6). Lower membrane exposure to the cleaning agent would result in slower membrane ageing and, consequently, increased membrane lifetime. As can be seen from TABLE 3.6, the lowest membrane exposure to the HCl solution occurred at a 0.20% w/w concentration. At this concentration, the estimated cleaning time for 90% cleaning efficiency was 1.2 h and the membrane exposure was 2,427 $mg \cdot L^{-1} \cdot h$ of HCl per cleaning procedure. The cleaning efficiency of 0.20% HCl was 46.8% in 30 min, which is relatively low. However, higher cleaning agent concentration led to much higher membrane exposure to HCl. For example, the membrane exposure to 1.00% HCl was 8,117 $mg \cdot L^{-1} \cdot h$, 70.1% higher than that at a concentration of 0.20%.

TABLE 3.6 – Estimated cleaning time and membrane exposure to HCl for 90% cleaning efficiency by each solution concentration studied

HCl Concentration (%w/w)	HCl Concentration (mg/L)	Cleaning Time for 90% Efficiency (min)	Membrane Exposure until 90% of Cleaning Efficiency (mg/L · h of HCl)
0.05	500	425	3,538
0.10	1,000	237	3,945
0.20	2,000	73	2,427
0.50	5,000	51	4,275
1.00	10,000	49	8,117

3.3.3 Membrane Ageing

TABLE 3.7 shows the measured membrane separation characteristics after long-term exposure to the AMD retentate, and to the AMD retentate plus periodic HCl cleaning solution. The 1.0% w/w HCl cleaning solution was used in this study to increase membrane

exposure to this acid and, thus, possible differences in membrane ageing. A continuous decline in water permeability was observed with increasing exposure time, up to an approximate value of 5.5 L/h·m^2·bar of water permeability for both experiments. Water permeability can decrease due to the adsorption of solutes onto the membrane surface, membrane pore blocking, concentration polarization, and cake formation. Because no pressure differential was applied in these experiments, concentration polarization and cake formation could be considered null and pore blocking minimal. Therefore, the adsorption of solutes onto the membrane surface was the main reason for the observed decrease in water permeability. The aim for using the HCl cleaning solution was to remove the sparingly soluble salts precipitated on the membrane surface, which are the main constituents of the fouling cake layer. Because the cake formation was null in this experiment, the periodic exposure to HCl was not expected to increase water permeability due to membrane cleaning. Hence, variations in the results from both tests were a result of interactions between the membrane and the HCl solution. Conversely, despite the decrease in water permeability over time, $MgSO_4$ rejection and glucose rejection did not show a steep decrease tendency (TABLE 3.7). After 150 days, $MgSO_4$ rejection decreased only 6% and 7%, respectively, for exposure to AMD and AMD plus periodic HCl, whereas glucose rejection decreased 3% and 4%, respectively, for exposure to AMD and AMD plus periodic HCl. This suggests that the adsorption of solutes onto the membrane surface did not strongly deteriorate the membrane selectivity, despite the decrease in water permeability.

TABLE 3.7 – NF270 separation characteristics with membrane exposure time

Exposure Time	Water Permeability (L/h·m²·bar)		$MgSO_4$ Rejection (%)		Glucose Rejection (%)	
	AMD	AMD + HCl	AMD	AMD + HCl	AMD	AMD + HCl
Initial	10.5	9.3	92.8	92.1	92.8	93.5
30 d	10.1	8.8	93.0	93.5	93.4	93.0
60 d	9.5	6.9	92.5	92.5	93.3	93.0
90 d	7.3	6.0	92.7	92.8	93.5	93.0
120 d	7.0	5.8	92.2	96.6	89.6	90.0
150 d	6.7	6.5	86.8	86.5	89.6	89.3
180 d	5.2	5.6	89.2	91.4	89.6	89.2
210 d	5.6	5.5	87.7	83.8	89.0	88.5
240 d	5.2	5.5	86.5	78.4	88.9	88.4
270 d	5.4	5.1	85.7	84.7	88.7	88.3

FIGURE 3.9 shows the SEM images obtained for: a) V-NF270, b) NF270 exposed to AMD (for 90 d), and c) NF270 exposed to AMD plus periodic HCl (for 90 d), each at two

magnifications. The membrane surface of the V-NF270 was very homogeneous with few irregularities. These irregularities became even less visible after the membrane was exposed to AMD retentate and AMD retentate plus periodic HCl solution.

FIGURE 3.9 – SEM images of: a) V-NF270; b) exposed to AMD (for 90 d); and c) exposed to AMD with periodic HCl (for 90 d), at x10,000 and x5,000 magnifications

a)

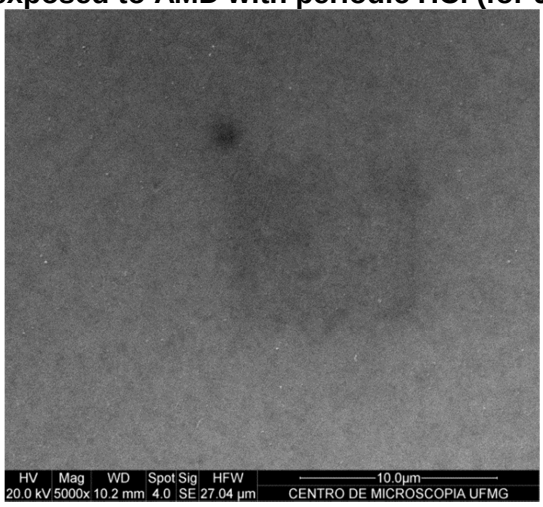

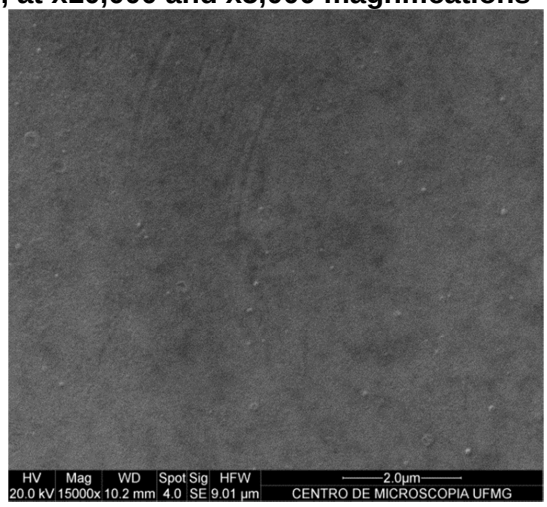

b)

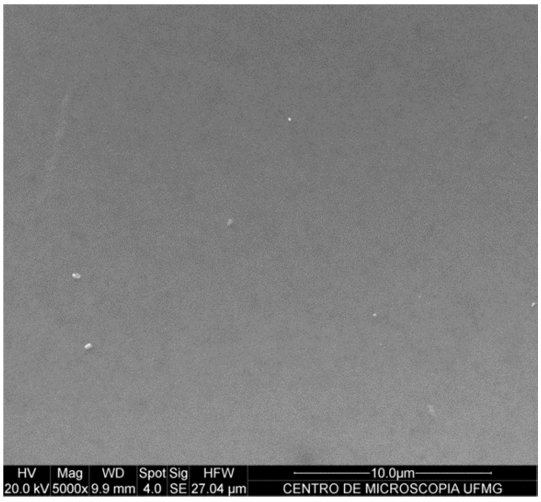

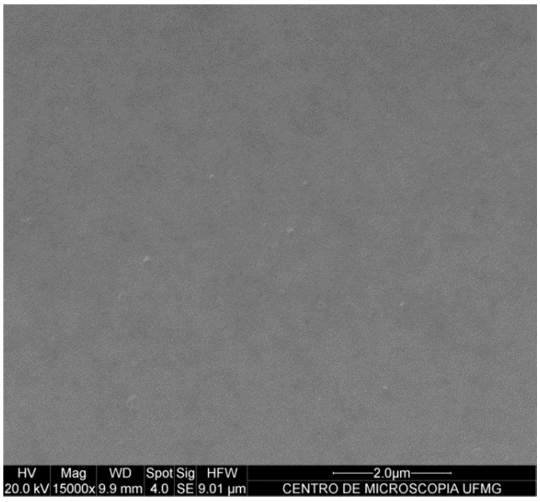

c)

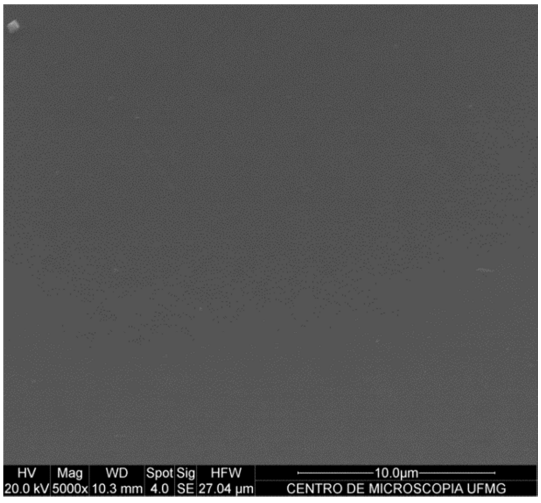

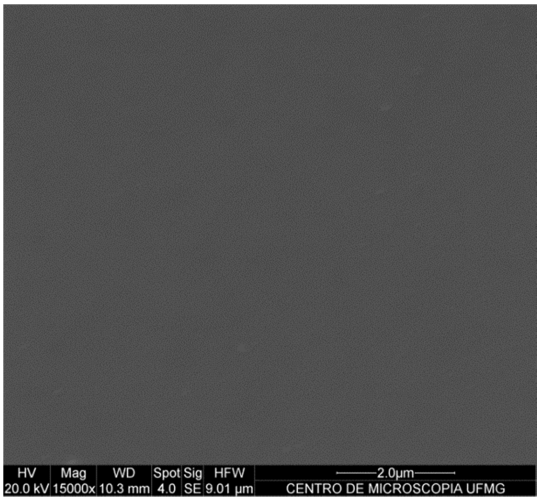

TABLE 3.8 shows the RMS roughness of the NF270 membranes exposed to AMD retentate and AMD retentate plus periodic HCl solution. Compared to the surface roughness of the V-NF270 membrane (5.18±0.71 nm), the surface roughness values of both the AMD-exposed membranes were higher. FIGURE 3.10 shows the AFM 3D images of the NF270 membranes exposed to AMD retentate [FIGURE 3.10(a)] and AMD retentate plus periodic HCl solution [FIGURE 3.10(b)]. A qualitative analysis of these images suggests that the membrane exposed only to AMD had a surface similar to the V-NF270 membrane [FIGURE 3.4(a)] but with higher peaks, which led to the higher RMS roughness value. This is consistent with the assumption that concentration polarization and cake formation were minimal during exposure without pressure. On the other hand, the membrane exposed to AMD and periodic HCl solution had a flatter surface with occasional deep valleys. This suggests the formation of an uneven fouling layer over the membrane surface, which could decrease the rejection of the membrane solutes and the water permeability.

TABLE 3.8 – Membrane surface roughness and water contact angle of the exposed NF270 membranes

Membrane	RMS Roughness (nm)	Water Contact Angle (°)
Exposed to AMD (270 d)	7.39±0.45	32.5±3.7
Exposed to AMD + periodic HCl (270 d)	6.78±0.81	38.9±3.7

The water contact angles of the membranes exposed to AMD retentate and AMD retentate plus periodic HCl solution are also shown in TABLE 3.8. As seen with the F-NF270 membrane (TABLE 3.3), the water contact angle of the NF270 membrane after exposure to AMD and AMD plus periodic HCl was higher than the V-NF270 membrane. These higher values corroborate the observed decrease in the water permeability of the exposed membranes. Moreover, the water contact angle of the membrane exposed to AMD plus periodic HCl was higher than that of the membrane exposed only to AMD. This opposed what was observed in SECTION 3.3.1. After membrane fouling during AMD treatment, the HCl solution increased the membrane hydrophilicity due to the removal of the cake-fouling layer, which is nonexistent in this experiment. Finally, the water contact angle of the FAC-NF270 membrane (TABLE 3.3) was close to that of the NF270 membrane exposed to AMD with periodic HCl. This could explain why the membrane did not return to its original state after the cleaning procedure.

FIGURE 3.10 – AFM images of the exposed NF270 membrane: a) to AMD (270 d); and b) to AMD + periodic HCl (270 d)

a)

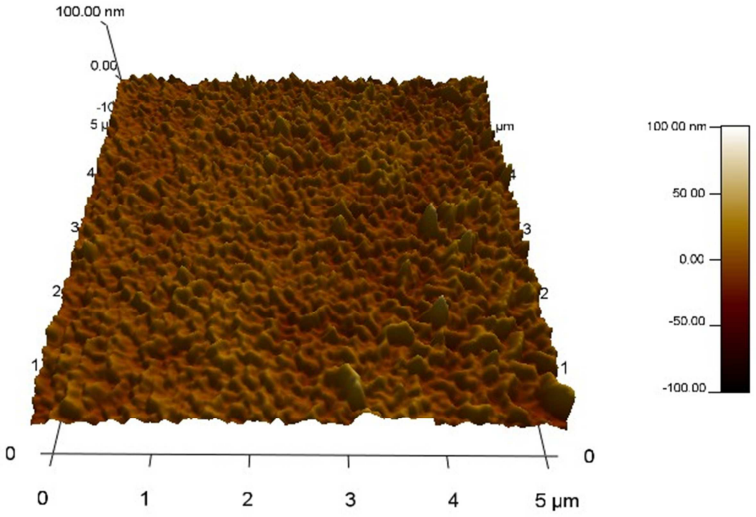

b)

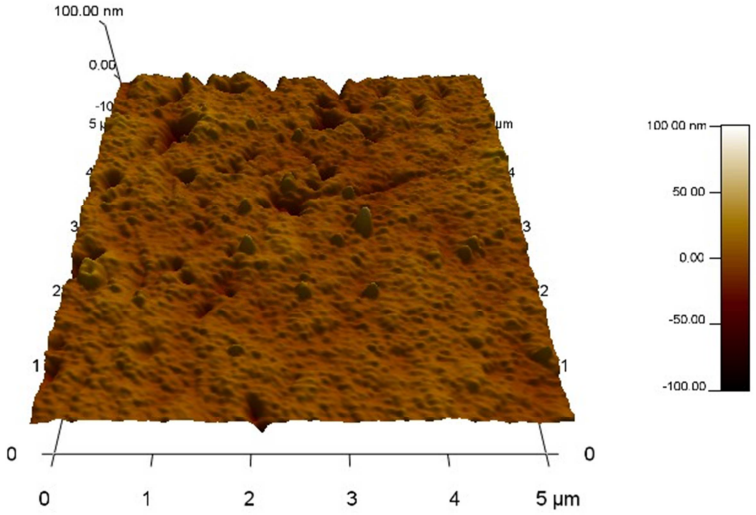

ATR/FTIR results for the V-NF270 membrane, the NF270 exposed to AMD (for 240 d), and the NF270 exposed to AMD with periodic HCl (for 240 d) are shown in FIGURE 3.11. Again, wavelength was from 400 to 2000 cm^{-1}, as no peaks were observed outside of this range. Similarly to the spectra of the F-NF270 and FAC-NF270, the spectra of the membranes exposed to AMD and AMD with periodic HCl had the same main peaks as the V-NF270 membrane. Very weak peaks were found on the membrane exposed only to AMD at wavelengths of 1558, 1487, and 988 cm^{-1}. This confirmed the stability of the NF270 membrane to AMD retentate and AMD retentate plus periodic HCl cleaning solution.

FIGURE 3.11 – ATR/FTIR spectra of NF270 membranes: V-NF270, exposed to AMD (for 240 d), and exposed to AMD plus periodic HCl (for 240 d)

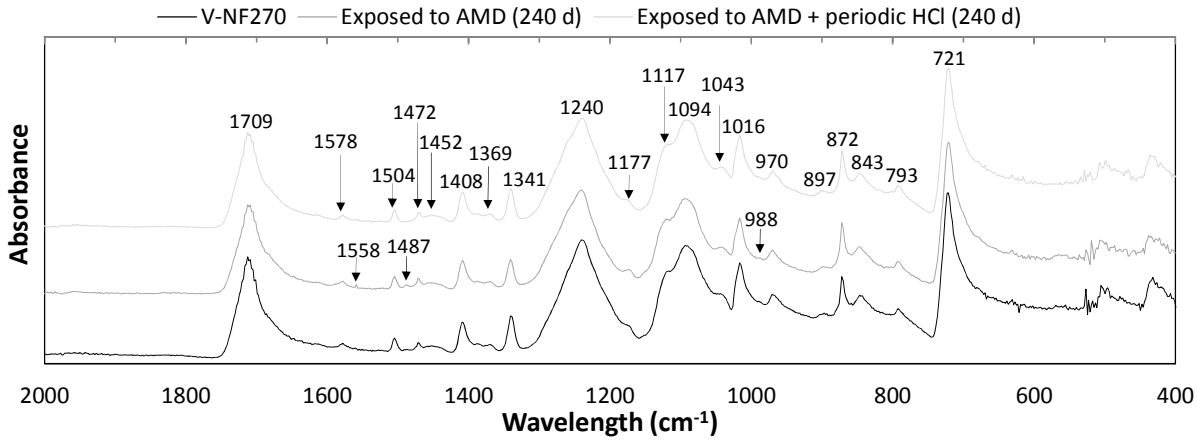

3.4 Conclusions

The main composition of the AMD are dissolved inorganic compounds which results mainly in inorganic fouling. The main cations found on the membrane surface were aluminum, arsenic, calcium, chromium, nickel, potassium, and sodium. Membrane fouling was responsible for a decrease in water permeability by 60% and could be partially removed by chemical cleaning. The aim of chemical cleaning optimization (in relation to cleaning agent type and solution concentration) was to minimize residual fouling and decrease cleaning procedure time. The cleaning tests showed that acidic solutions are more efficient cleaning solutions for AMD foulants than alkaline or surfactant solutions. Among the acidic solutions, the best cleaning efficiency (73.5%) was obtained with HCl 0.2% w/w and the estimated cost per cleaning procedure with HCl was economically viable. Next, different HCl concentrations were evaluated. The lowest membrane exposure occurred at 0.20% w/w concentration (efficiency of 46.8% after 30 min cleaning). Membrane ageing by AMD retentate and AMD retentate with periodic HCl solution decreased the NF270 water permeability; however, $MgSO_4$ and glucose rejection were still high after 270 d of exposure. ATR/FTIR spectra of all the tested membranes assessed in this study were very similar, with strong peaks at the same wavelengths. This suggests that the bonds of the chemicals on the membrane surface were not altered by any of the treatments tested.

4 CHAPTER

SUMMARY OF EXPERIMENTAL PROGRESS

In this study, acid mine drainage (AMD) treatment by membrane separation processes (MSP) was investigated.

In Chapter 2, the influence of operational parameters, namely, effluent pretreatment, nanofiltration (NF) and reverse osmosis (RO) commercial membranes, effluent pH, and water recovery rate was evaluated. Since effluent pretreatment improved the final permeate quality and due to the highly variable characteristics of this effluent, microfiltration (MF) or better was deemed appropriate prior to NF/RO treatment. Among the NF and RO commercial membranes tested, NF showed higher potential for AMD treatment. The best NF membranes tested were the NF90 (highest retention efficiency), and the NF270 (highest permeate flux). The feed effluent pH effects the effluent permeate flux, the membrane-fouling tendency, the solutes retention efficiency. The best operational condition was obtained at pH 5.5 with the NF270 membrane. It had the lowest fouling tendency, highest permeate flux by water flux (85.3%), and high sulfate retention efficiency (86.1%). The maximum water recovery rate (RR) at this condition was 60%. Above this value, a sharper decrease in retention efficiency and permeate flux were observed.

Therefore, as a result of this work, it was found that the best treatment route for gold AMD by MSP is: adjust the feed pH to 5.5; pretreat with microfiltration or ultrafiltration; treat with the nanofiltration membrane NF270 until a water recovery rate of 60%. The capital cost estimated for the treatment of 15 m^3/h of AMD by a UF-NF system was US$ 131,250.00, and the estimated total operational cost was 0.257 US$/$m^3$ of effluent. The retentate generated during AMD treatment is more concentrated in dissolved solids than the original effluent. Therefore, sulfate precipitation as $CaSO_4$ or calcium precipitation as $CaCO_3$ would be more efficient. Moreover, after precipitation, a second stage of nanofiltration could be carried out to increase water recovery.

In Chapter 3, the inorganic fouling formed during AMD treatment was analyzed and the main cations found on the membrane surface were aluminum, arsenic, calcium, chrome, nickel, potassium and sodium. These foulants could be partially removed by chemical cleaning and its optimization aimed to minimize residual fouling and decrease cleaning procedure time. The best cleaning solution evaluated to remove the AMD foulants was hydrochloric acid (cleaning efficiency of 73.5% at 0.20% w/w) and its estimate cost per cleaning procedure made it economically viable. Moreover, the lowest membrane exposure to acid occurred at

0.20% w/w concentration which was then considered the best cleaning condition. Membrane ageing by AMD retentate, and AMD retentate plus periodical HCl cleaning solution decreased the NF270 water permeability; however, $MgSO_4$ and glucose rejection were still high after 270 days of exposure. ATR/FTIR spectra of the membranes assessed in this work were very similar, which suggests that the chemicals bonds on the membrane surface were not altered by either treatment or exposure to AMD and HCl.

5 CHAPTER

SUGGESTIONS FOR FUTURE WORK

The following studies are suggested for future research:

- The evaluation of calcium and/or sulfate precipitation from the AMD retentate. Depending on these pollutants removal efficiency, the precipitation step could be an intermediate process, allowing a second stage of nanofiltration;

- The increase of maximum water recovery with a second stage of nanofiltration (after an intermediate precipitation step) and the respective increase in treatment cost;

- The influence of solution temperature in AMD nanofiltration in terms of permeate flux and retention efficiency;

- The influence of solution temperature in chemical cleaning procedure, cleaning efficiency and membrane ageing;

- In a pilot scale unit, investigate the influence of other operational parameters in AMD nanofiltration. The main parameters to be investigated are crossflow velocity and transmembrane pressure;

- Evaluate the continuous operation of the optimized treatment in a pilot scale unit.

BIBLIOGRAPHY

AL-RASHDI, B. A. M.; JOHNSON, D. J.; HILAL, N. Removal of heavy metal ions by nanofiltration. **Desalination,** v. 315, p. 2-17, 2013. ISSN 0011-9164.

AL-ZOUBI, H. et al. Optimization study for treatment of acid mine drainage using membrane technology. **Separation Science and Technology,** v. 45, n. 14, p. 2004-2016, 2010. ISSN 0149-6395.

ANAWAR, H. M. Impact of climate change on acid mine drainage generation and contaminant transport in water ecosystems of semi-arid and arid mining areas. **Physics and Chemistry of the Earth, Parts A/B/C,** v. 58, p. 13-21, 2013. ISSN 1474-7065.

ANG, W. S. et al. Chemical cleaning of RO membranes fouled by wastewater effluent: achieving higher efficiency with dual-step cleaning. **Journal of Membrane Science,** v. 382, n. 1, p. 100-106, 2011. ISSN 0376-7388.

APHA. **Standard methods for the examination of water and wastewater**. ASSOCIATION, A. P. H. Washington: APHA 2005.

BADER, M. S. H. Sulfate removal technologies for oil fields seawater injection operations. **Journal of Petroleum Science and Engineering,** v. 55, n. 1, p. 93-110, 2007. ISSN 0920-4105.

BAKER. **Membrane technology and applications**. 3rd. A John Wiley & Sons, Ltd., Publication, 2012. ISBN 9780470743720.

BALANNEC, B. et al. Comparative study of different nanofiltration and reverse osmosis membranes for dairy effluent treatment by dead-end filtration. **Separation and Purification Technology,** v. 42, n. 2, p. 195-200, 2005. ISSN 1383-5866.

BALANYÀ, T. et al. Separation of metal ions and chelating agents by nanofiltration. **Journal of Membrane Science,** v. 345, n. 1, p. 31-35, 2009. ISSN 0376-7388.

BARGEMAN, G. et al. Nanofiltration as energy-efficient solution for sulfate waste in vacuum salt production. **Desalination,** v. 245, n. 1, p. 460-468, 2009. ISSN 0011-9164.

BARNHISEL, R. I.; DARMODY, R. G.; DANIELS, W. L. Acid mine drainage control and treatment. In: (Ed.). **Reclamation of Drastically Disturbed Lands**: American Society of Agronomy, Crop Science Society of America, Soil Science Society of America, 2000. p.131-168. ISBN 978-0-89118-233-7.

BI, F. et al. Discussion on calculation of maximum water recovery in nanofiltration system. **Desalination,** v. 332, n. 1, p. 142-146, 2014. ISSN 0011-9164.

CARVALHO, A. L. et al. Separation of potassium clavulanate and potassium chloride by nanofiltration: Transport and evaluation of membranes. **Separation and Purification Technology,** v. 83, p. 23-30, 2011. ISSN 1383-5866.

CHAKRAVORTY, B.; LAYSON, A. Ideal feed pretreatment for reverse osmosis by continuous microfiltration. **Desalination,** v. 110, n. 1, p. 143-149, 1997. ISSN 0011-9164.

CHEN, W.-H. et al. Therapeutic nanomedicine based on dual-intelligent functionalized gold nanoparticles for cancer imaging and therapy *in vivo*. **Biomaterials,** v. 34, n. 34, p. 8798-8807, 2013. ISSN 0142-9612.

COSTA, A. R.; DE PINHO, M. N. Performance and cost estimation of nanofiltration for surface water treatment in drinking water production. **Desalination,** v. 196, n. 1, p. 55-65, 2006. ISSN 0011-9164.

COSTELLO, C. Acid mine drainage: innovative treatment technologies. **Washington DC: US Environmental Protection Agency Office of Solid Waste and Emergency Response**, 2003.

DALWANI, M. et al. Effect of pH on the performance of polyamide/polyacrylonitrile based thin film composite membranes. **Journal of Membrane Science,** v. 372, n. 1, p. 228-238, 2011. ISSN 0376-7388.

DIAO, Z. et al. Silane-based coatings on the pyrite for remediation of acid mine drainage. **Water research,** v. 47, n. 13, p. 4391-4402, 2013. ISSN 0043-1354.

DNPM. **Economia mineral do Brasil**. Brasília - DF - Brasil. 2009

DNPM. **Sumário Mineral**. Brasília - DF - Brasil 2014.

DO, V. T. et al. Degradation of polyamide nanofiltration and reverse osmosis membranes by hypochlorite. **Environmental science & technology,** v. 46, n. 2, p. 852-859, 2012. ISSN 0013-936X.

DRIOLI, E.; GIORNO, L. **Membrane operations: innovative separations and transformations**. Wiley-VCH, 2009. ISBN 3527320385.

DUBOIS, M. et al. Colorimetric method for determination of sugars and related substances. **Analytical chemistry,** v. 28, n. 3, p. 350-356, 1956. ISSN 0003-2700.

FORNARELLI, R.; MULLETT, M.; RALPH, D. Factors influencing nanofiltration of acid mine drainage. 2013.

FUJIOKA, T. et al. Effects of feed solution characteristics on the rejection of N-nitrosamines by reverse osmosis membranes. **Journal of Membrane Science,** v. 409, p. 66-74, 2012. ISSN 0376-7388.

GABELICH, C. J. et al. High-recovery reverse osmosis desalination using intermediate chemical demineralization. **Journal of Membrane Science,** v. 301, n. 1, p. 131-141, 2007. ISSN 0376-7388.

GFMS. **GFMS Gold Survey**. Thomson Reuters. London (UK). 2014

GHOSH, A. K. et al. Impacts of reaction and curing conditions on polyamide composite reverse osmosis membrane properties. **Journal of Membrane Science,** v. 311, n. 1, p. 34-45, 2008. ISSN 0376-7388.

GORENFLO, A.; VELAZQUEZ-PADRON, D.; FRIMMEL, F. H. Nanofiltration of a German groundwater of high hardness and NOM content: performance and costs. **Desalination,** v. 151, n. 3, p. 253-265, 2002. ISSN 0011-9164.

GRANDE, J. et al. Overall hydrochemical characterization of the Iberian Pyrite Belt. Main acid mine drainage-generating sources (Huelva, SW Spain). **Journal of hydrology,** v. 390, n. 3, p. 123-130, 2010. ISSN 0022-1694.

HENTHORNE, L.; BOYSEN, B. State-of-the-art of reverse osmosis desalination pretreatment. **Desalination,** v. 356, p. 129-139, 2015. ISSN 0011-9164.

HILAL, N. et al. Characterisation of nanofiltration membranes using atomic force microscopy. **Desalination,** v. 177, n. 1, p. 187-199, 2005. ISSN 0011-9164.

JAMALY, S. et al. A short review on reverse osmosis pretreatment technologies. **Desalination,** v. 354, p. 30-38, 2014. ISSN 0011-9164.

JOHNSON, D. B.; HALLBERG, K. B. Acid mine drainage remediation options: a review. **Science of the total environment,** v. 338, n. 1, p. 3-14, 2005. ISSN 0048-9697.

JUDD, S. **The MBR book: principles and applications of membrane bioreactors for water and wastewater treatment**. Elsevier, 2010. ISBN 0080967671.

KARABELAS, A. J.; KARANASIOU, A.; MITROULI, S. T. Incipient membrane scaling by calcium sulfate during desalination in narrow spacer-filled channels. **Desalination,** v. 345, p. 146-157, 2014. ISSN 0011-9164.

KLÜPFEL, A. M.; FRIMMEL, F. H. Nanofiltration of river water—fouling, cleaning and micropollutant rejection. **Desalination,** v. 250, n. 3, p. 1005-1007, 2010. ISSN 0011-9164.

LALIA, B. S. et al. A review on membrane fabrication: Structure, properties and performance relationship. **Desalination,** v. 326, p. 77-95, 2013. ISSN 0011-9164.

LI, N. N. et al. **Advanced membrane technology and applications**. John Wiley & Sons, 2011. ISBN 1118211545.

LIU, M. et al. Comparison of reverse osmosis and nanofiltration membranes in the treatment of biologically treated textile effluent for water reuse. **Desalination,** v. 281, p. 372-378, 2011. ISSN 0011-9164.

MME. **Relatório Técnico 28 - Perfil do Ouro**. 2009

MOHAPATRA, B. R. et al. Tracking the prokaryotic diversity in acid mine drainage-contaminated environments: a review of molecular methods. **Minerals Engineering,** v. 24, n. 8, p. 709-718, 2011. ISSN 0892-6875.

MULLETT, M.; FORNARELLI, R.; RALPH, D. Nanofiltration of mine water: impact of feed pH and membrane charge on resource recovery and water discharge. **Membranes,** v. 4, n. 2, p. 163-180, 2014.

NOBLE, R. D.; STERN, S. A. **Membrane separations technology: principles and applications**. Elsevier, 1995. ISBN 0080536182.

NORGATE, T.; HAQUE, N. Using life cycle assessment to evaluate some environmental impacts of gold production. **Journal of Cleaner Production,** v. 29, p. 53-63, 2012. ISSN 0959-6526.

ONN, A. H.; WOODLEY, A. A discourse analysis on how the sustainability agenda is defined within the mining industry. **Journal of Cleaner Production,** v. 84, p. 116-127, 2014. ISSN 0959-6526.

PEARCE, G. K. UF/MF pre-treatment to RO in seawater and wastewater reuse applications: a comparison of energy costs. **Desalination,** v. 222, n. 1, p. 66-73, 2008. ISSN 0011-9164.

REGULA, C. et al. Chemical cleaning/disinfection and ageing of organic UF membranes: a review. **Water research,** v. 56, p. 325-365, 2014. ISSN 0043-1354.

RICCI, B. C. et al. Integration of nanofiltration and reverse osmosis for metal separation and sulfuric acid recovery from gold mining effluent. **Separation and Purification Technology,** v. 154, p. 11-21, 2015. ISSN 1383-5866.

ROBLES-ARENAS, V. et al. Sulphide-mining impacts in the physical environment: Sierra de Cartagena–La Unión (SE Spain) case study. **Environmental Geology,** v. 51, n. 1, p. 47-64, 2006. ISSN 0943-0105.

SCHMID, G.; CORAIN, B. Nanoparticulated gold: syntheses, structures, electronics, and reactivities. **European Journal of Inorganic Chemistry,** v. 2003, n. 17, p. 3081-3098, 2003. ISSN 1099-0682.

SEDIN, D. L.; ROWLEN, K. L. Influence of tip size on AFM roughness measurements. **Applied surface science,** v. 182, n. 1, p. 40-48, 2001. ISSN 0169-4332.

SETHI, S.; WIESNER, M. R. Cost modeling and estimation of crossflow membrane filtration processes. **Environmental engineering science,** v. 17, n. 2, p. 61-79, 2000. ISSN 1092-8758.

SHAHALAM, A. M.; AL-HARTHY, A.; AL-ZAWHRY, A. Feed water pretreatment in RO systems: unit processes in the Middle East. **Desalination,** v. 150, n. 3, p. 235-245, 2002. ISSN 0011-9164.

SHEN, J. et al. Techno-economic analysis of resource recovery of glyphosate liquor by membrane technology. **Desalination,** v. 342, p. 118-125, 2014. ISSN 0011-9164.

SIERRA, C.; SAIZ, J. R. Á.; GALLEGO, J. L. R. Nanofiltration of Acid Mine Drainage in an Abandoned Mercury Mining Area. **Water, Air, & Soil Pollution,** v. 224, n. 10, p. 1-12, 2013. ISSN 0049-6979.

SIMON, A. et al. Effects of caustic cleaning on pore size of nanofiltration membranes and their rejection of trace organic chemicals. **Journal of Membrane Science,** v. 447, p. 153-162, 2013. ISSN 0376-7388.

SIMON, A.; PRICE, W. E.; NGHIEM, L. D. Effects of chemical cleaning on the nanofiltration of pharmaceutically active compounds (PhACs). **Separation and Purification Technology,** v. 88, p. 208-215, 2012. ISSN 1383-5866.

SIMON, A.; PRICE, W. E.; NGHIEM, L. D. Impact of chemical cleaning on the nanofiltration of pharmaceutically active compounds (PhACs): The role of cleaning temperature. **Journal of the Taiwan Institute of Chemical Engineers,** v. 44, n. 5, p. 713-723, 2013. ISSN 1876-1070.

SOHRABI, M. R. et al. Chemical cleaning of reverse osmosis and nanofiltration membranes fouled by licorice aqueous solutions. **Desalination,** v. 267, n. 1, p. 93-100, 2011. ISSN 0011-9164.

TAB – TECHNICAL APPLICATION BULLETIM. **Hydranautics, Chemical pretreatment of RO and NF**. TAB n. 111, rev. C, NITTO DENKO, N. 2008.

TANG, C. Y.; KWON, Y.-N.; LECKIE, J. O. Effect of membrane chemistry and coating layer on physiochemical properties of thin film composite polyamide RO and NF membranes: I. FTIR and XPS characterization of polyamide and coating layer chemistry. **Desalination,** v. 242, n. 1, p. 149-167, 2009. ISSN 0011-9164.

TANNINEN, J. et al. Long-term acid resistance and selectivity of NF membranes in very acidic conditions. **Journal of membrane science,** v. 240, n. 1, p. 11-18, 2004. ISSN 0376-7388.

TCHOBANOGLOUS, G.; BURTON, F. L.; STENSEL, H. D. **Wastewater Engineering: Treatment and Reuse**. 4th Edition. New York: McGraw-Hill Science/Engineering/Math, 2003. ISBN 978-0070418783.

TEIXEIRA, M. R.; ROSA, M. J.; NYSTRÖM, M. The role of membrane charge on nanofiltration performance. **Journal of Membrane Science,** v. 265, n. 1, p. 160-166, 2005. ISSN 0376-7388.

TRINDADE, R. E.; BARBOSA FILHO, O. **Extração de ouro: princípios, tecnologia e meio ambiente**. CETEM, 2002.

TU, K. L.; NGHIEM, L. D.; CHIVAS, A. R. Coupling effects of feed solution pH and ionic strength on the rejection of boron by NF/RO membranes. **Chemical Engineering Journal,** v. 168, n. 2, p. 700-706, 2011. ISSN 1385-8947.

VANYSACKER, L.; BERNSHTEIN, R.; VANKELECOM, I. F. J. Effect of chemical cleaning and membrane aging on membrane biofouling using model organisms with increasing complexity. **Journal of Membrane Science,** v. 457, p. 19-28, 2014. ISSN 0376-7388.

WANG, Z. et al. Studies on nanofiltration membrane fouling in the treatment of water solutions containing humic acids. **Desalination,** v. 178, n. 1, p. 171-178, 2005. ISSN 0011-9164.

WEI, J. et al. Comparison of NF-like and RO-like thin film composite osmotically-driven membranes—implications for membrane selection and process optimization. **Journal of Membrane Science,** v. 427, p. 460-471, 2013. ISSN 0376-7388.

WEI, X. et al. Advanced treatment of a complex pharmaceutical wastewater by nanofiltration: membrane foulant identification and cleaning. **Desalination,** v. 251, n. 1, p. 167-175, 2010. ISSN 0011-9164.

YU, S. et al. Impacts of membrane properties on reactive dye removal from dye/salt mixtures by asymmetric cellulose acetate and composite polyamide nanofiltration membranes. **Journal of Membrane Science,** v. 350, n. 1-2, p. 83-91, 2010. ISSN 03767388.